
Supporting Information for

Original article

Self-assembling, pH-responsive nanoflowers for inhibiting PAD4 and neutrophil extracellular trap formation and improving the tumor immune microenvironment

Di Zhu^{a,b,†}, Yu Lu^{a,b,†}, Lin Gui^{a,b}, Wenjing Wang^c, Xi Hu^d, Su Chen^e, Yanming Wang^f, Yuji Wang^{a,b,*}

^aDepartment of Medicinal Chemistry, College of Pharmaceutical Sciences of Capital Medical University, Beijing 100069, China

^bBeijing Area Major Laboratory of Peptide and Small Molecular Drugs, Engineering Research Center of Endogenous Prophylactic of Ministry of Education of China, Beijing Laboratory of Biomedical Materials, Beijing 100069, China

^cBeijing Institute of Hepatology, Beijing Youan Hospital, Capital Medical University, Beijing 100069, China.

^dQuantum Design China Ltd., Universal Business Park, Beijing 100015, China

^eLaboratory of Biomaterials and Biomechanics, Beijing Key Laboratory of Tooth Regeneration and Function Reconstruction, School of Stomatology, Capital Medical University, Beijing 100050, China

^fSchool of Life Sciences, Henan University, Kaifeng 475004, China

Received 9 July 2021; received in revised form 13 September 2021; accepted 10 October 2021

*Corresponding author. Tel./fax: +86 10 83911530.

E-mail address: wangyuji@ccmu.edu.cn (Yuji Wang).

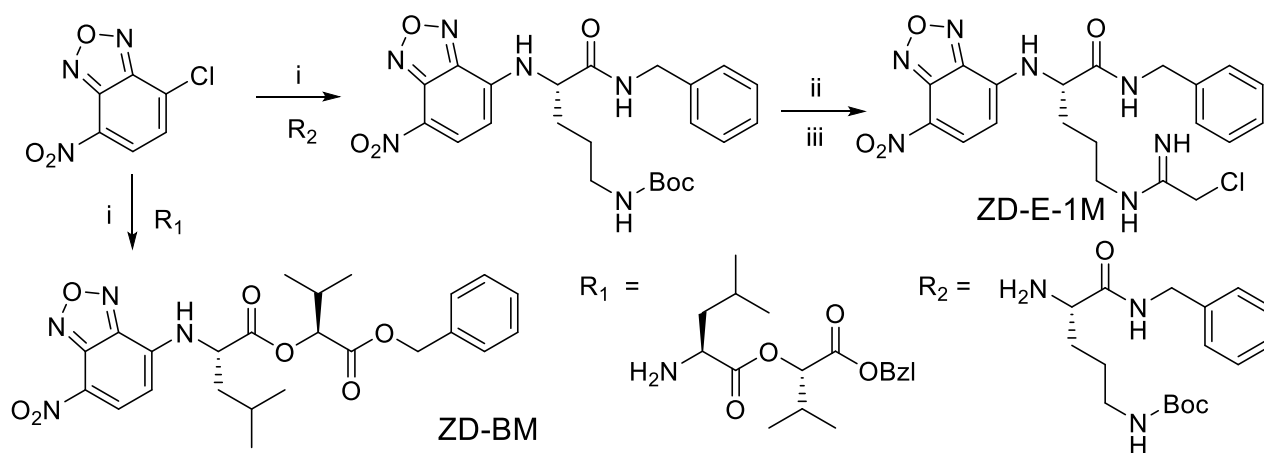
†These authors made equal contributions to this work.

Running title: Nanoflowers inhibiting PAD4, NETs and regulating tumor immunity

Scheme S1 Synthesis route of ZD-BM and ZD-E-1M; Figs. S1–S25 The characteristic information of MS, ¹H NMR, ¹³C NMR, IR, HPLC, UV and fluorescence spectrum; Fig. S26 2D schematic diagram of docking model of (A) ZD-E-1M and (B) ZD-BM with PAD4; Fig. S27 PAD4 inhibition activity assessed by a colorimetric method. (A) PAD4 inhibition ratio of YW3-56, ZD-BM and ZD-E-1M. (B) The experimental workflow of PAD4 inhibition determination. (C) Mechanism of ZD-E-1M inhibiting PAD4; Fig. S28 Nano self-assembly characterization. (A–D) Size distribution of ZD-B and ZD-E-1 at pH 6.5 and pH 7.4 in TEM photos analyzed by ImageJ. (E–F) Size and zeta potential changes with concentration of ZD-E-1; Fig. S29 Nano self-assembly properties of ZD-B. (A–B) The critical aggregation concentration (CAC) at pH 7.4 and pH 6.5. (C) Drug release curve at pH 7.4 and pH 6.5; Fig. S30 FTMS spectra and NOSEY 2D NMR in acid solvent. (A–B) FTMS spectra of ZD-B and ZD-E-1 at pH 6.5. (C–D) NOSEY 2D NMR of ZD-B and ZD-E-1 at pH 6.5. (E–F) Molecular

dynamics simulation of ZD-B and ZD-E-1 in self-assembled nano-units in acidic solution; Fig. S31 Uptake behavior and uptake pathway. (A) The uptake of ZD-E-1 was measured by HPLC-MS (SCIEX) on 4T1 and HL7702 cells at different pH values for 48 h. (B) Flow cytometry (BD) measured the uptake of ZD-B and ZD-E-1 by 4T1 cells at different pH values for 48 h. (C) Flow cytometry (BD) measured the uptake pathway of ZD-E-1 by 4T1 cells; Fig. S32 (A) The levels of H3cit and subcellular colocalization of ZD-E-1 and H3cit in 4T1 cells determined by CLSM (Leica); (B–C) Protein expression in 4T1 cells treated with ZD-E-1 (10 $\mu\text{mol/L}$, 5 $\mu\text{mol/L}$, 1 $\mu\text{mol/L}$) evaluated by immunoblotting and gray value analysis; Fig. S33 The nanotoxicity of ZD-E-1 on 4T1 orthotopic tumor-bearing mice. (A) Histological analysis of main organs by HE staining; (B–E) ALT, AST, creatinine, and urea levels in serum; Fig. S34 Gating Hierarchy Plots; Fig. S35 The nanotoxicity of ZD-E-1 on LLC tumor-bearing mice. (A) Body weight of LLC tumor-bearing mice; (B–F) main organs weight of LLC tumor-bearing mice; (G–J) ALT, AST, creatinine, and urea levels in serum; Fig. S36 The serum stability (A) and pharmacokinetics (B) determined by HPLC-MS (SCIEX); Table S1 Molecular docking of compounds toward active site of PAD4 enzyme; Table S2 IC_{50} values of compounds determined after 48h incubation; Table S3 Penal of mass cytometry. Synthesis procedure and experimental methods are also shown in Supporting Information.

1. Synthesis



Scheme S1 Synthesis of ZD-BM and ZD-E-1M. Regents and conditions. i. DIPEA, methanol anhydrous; ii. 2 mol/L HCl/EA; iii. 2-chloroacetylamine ethyl ester, DIPEA, methanol anhydrous.

1.1. Synthesis of ZD-BM

(S)-1-(benzyloxy)-3-methyl-1-oxobutan-2-yl(*S*)-2-((λ^2 -chloranyl)- λ^4 -azanyl)-4-methylpentanoate (*Boc-Leu-Val-OBzl*).

A mixture of *Boc-Leu* (2.490 g, 10 mmol) and *Val-OBzl* (2.484 g, 12 mmol), DCC (2.472 g, 12 mmol), HOBt (1.620 g, 12 mmol), NMM (3.4 mL, 30 mmol) in anhydrous tetrahydrofuran (THF, 100 mL) was stirred at room temperature for 8 h. TLC ($\text{CH}_2\text{Cl}_2:\text{CH}_3\text{OH} = 30:1$, $R_f = 0.38$) was used to monitor the process. The solvent was evaporated in vacuo. The residue was dissolved in 60 mL of EA. And the solution was washed successively with saturated aqueous solution of NaHCO_3 (20 mL \times 3), saturated aqueous solution of NaCl (20 mL \times 3), 5% aqueous solution of KHSO_4 (20 mL \times 3), saturated aqueous solution of NaCl (20 mL \times 3). Then the solution was dried over anhydrous Na_2SO_4 . After filtration, the filtrate was evaporated in vacuo and the crude materials were purified by flash chromatography (column type: SNAP KP-Sil Cartridge; 5% $\text{CH}_3\text{OH}/\text{CH}_2\text{Cl}_2$) to give *Boc-Leu-Val-OBzl* (4.050 g, 96.4%) as a white solid. ESI-MS (m/z): 419.7 $[\text{M}-\text{H}]^-$; ^1H NMR (300 MHz, $\text{DMSO}-d_6$): δ (ppm) = 7.97 (d, $J = 8.2$ Hz, 1H), 7.36 (m, 5H), 6.90 (d, $J = 8.5$ Hz, 1H), 5.12 (t, $J = 4.2$ Hz, 2H), 4.25 (dd, $J = 8.2$ Hz, 6.3 Hz, 1H), 4.06 (dd, $J = 5.7$ Hz, 3.4 Hz, 1H), 2.08 (m, $J = 6.6$ Hz, 2H), 1.58 (m, 1H), 1.41 (m, 2H), 1.37 (s, 9H), 0.85 (m, 12H). Then it was stirred with 2 mol/L HCl/EA (20 mL) at 0 °C for 2 h. The solvent was evaporated in vacuo with dried EA (10 mL \times 3) and diethyl ether (10 mL \times 1) to give the intermediate *LV-OBzl* (3.330 g, 96.9%) as a white solid. ESI-MS (m/z): 321.3 $[\text{M}+\text{H}]^+$.

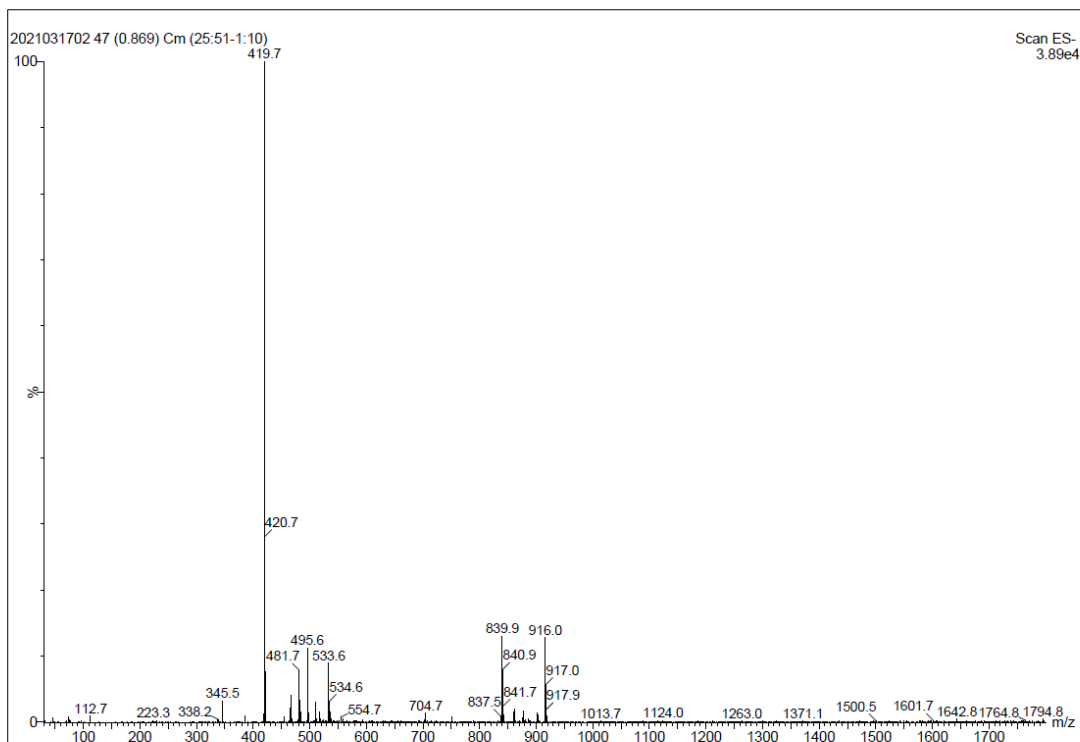


Figure S1 ESI-MS of Boc-Leu-Val-OBzl.

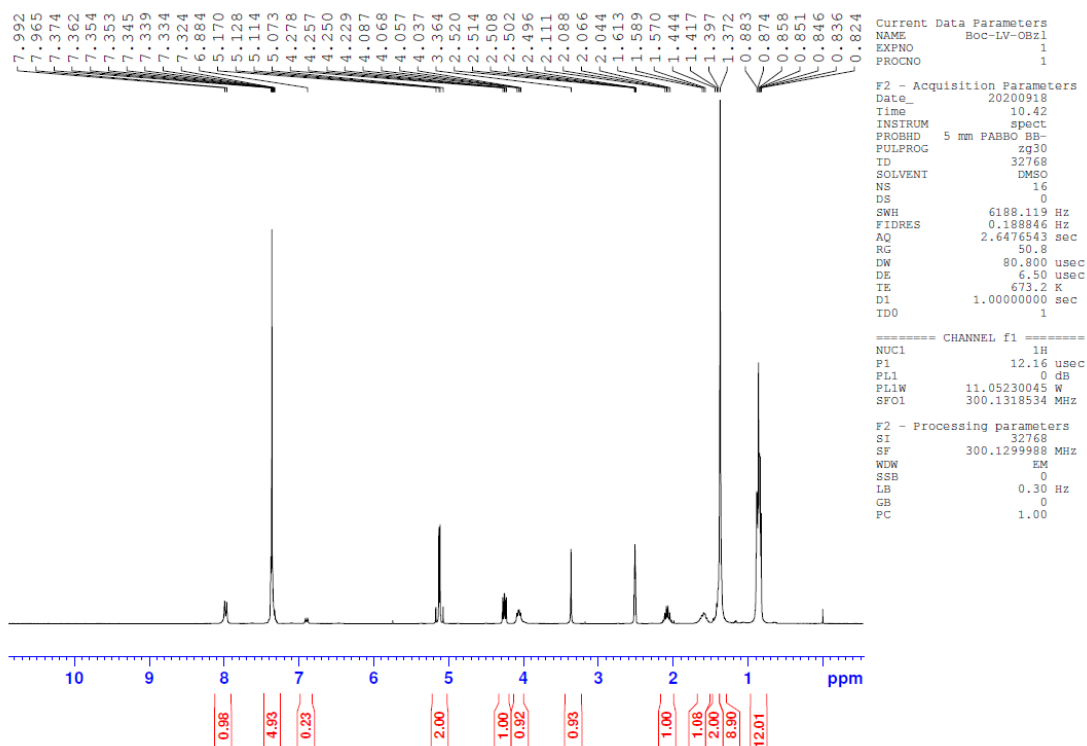


Figure S2 ^1H NMR of Boc-Leu-Val-OBzl.

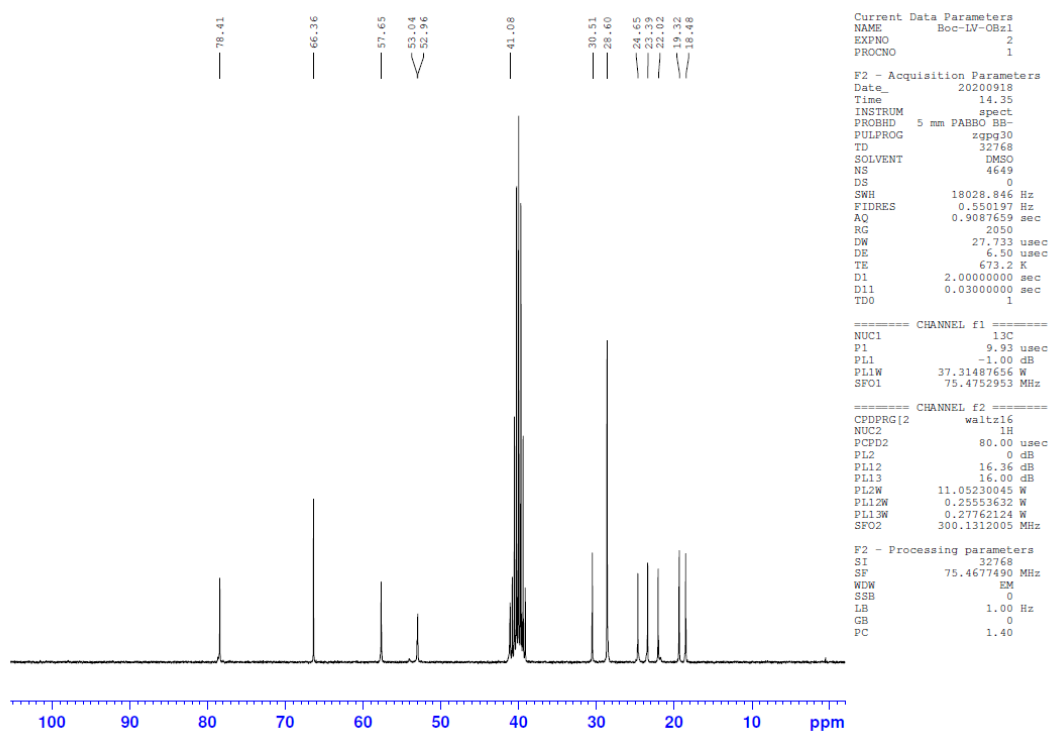


Figure S3 ^{13}C NMR of Boc-Leu-Val-OBzl.

1.1.2. Synthesis of (S)-1-(benzyloxy)-3-methyl-1-oxobutan-2-yl(7-nitrobenzo[c][1,2,5]oxadiazol-4-yl)-L-leucinate (ZD-BM).

A mixture of LV-OBzl (1.854 g, 6 mmol), 4-chloro-7-nitro-1,2,3-benzoxadiazole (0.998 g, 5 mmol) and DIPEA (5.22 mL, 6 mmol) in methanol anhydrous (100 mL) was stirred at room temperature for 8 h. TLC (PE:EA = 1:1, R_f = 0.25) was used to monitor the process. The solvent was evaporated in vacuo and the crude material was purified by flash chromatography (column type: SNAP KP-Sil Cartridge; 50% EA/PE) to afford the target ZD-BM (1.600 g, 66.2%) as a yellow powder, m.p. 147.4–149.1 °C; n_D^{20} = -77.5, (C 0.1 mg/mL, CH₃OH); FT-MS (m/z): 482.2045 [M-H]⁻; ^1H NMR (300 MHz, DMSO-*d*₆): δ (ppm) = 9.38 (s, 1H), 8.58 (s, 1H), 8.52(d, J = 8.9 Hz, 1H), 7.34 (s, 5H), 6.42 (s, 1H), 5.12 (d, J = 4.1 Hz, 2H), 4.52 (s, 1H), 4.27 (t, J = 6.4 Hz, 1H), 2.11 (m, 1H), 1.91 (s, 1H), 1.72 (s, 1H), 1.61 (s, 1H), 0.91 (t, J = 5.7 Hz, 6H), 0.86 (d, J = 6.3 Hz, 6H); ^{13}C NMR (75 MHz, DMSO-*d*₆): δ (ppm) = 171.4, 144.7, 137.9, 136.2, 128.8, 128.6, 128.5, 122.3, 100.1, 66.5, 58.0, 56.2, 30.3, 24.8, 23.3, 22.0, 19.4, 18.6.

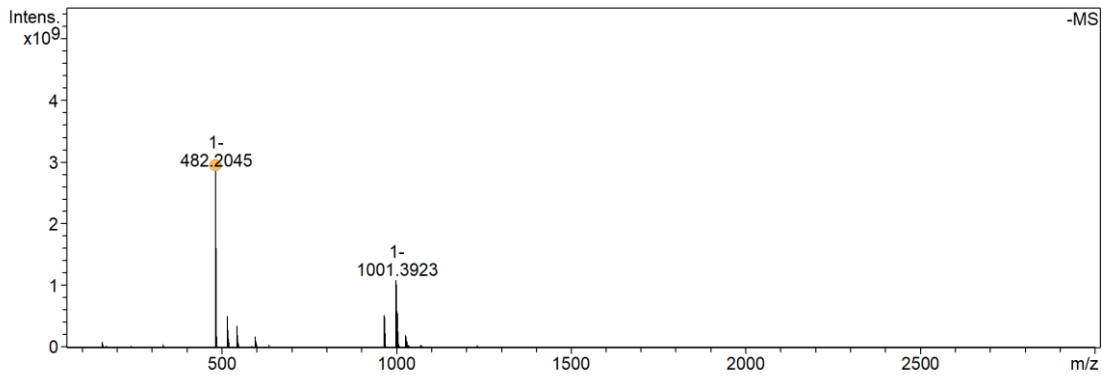


Figure S4 FT-MS of ZD-BM.

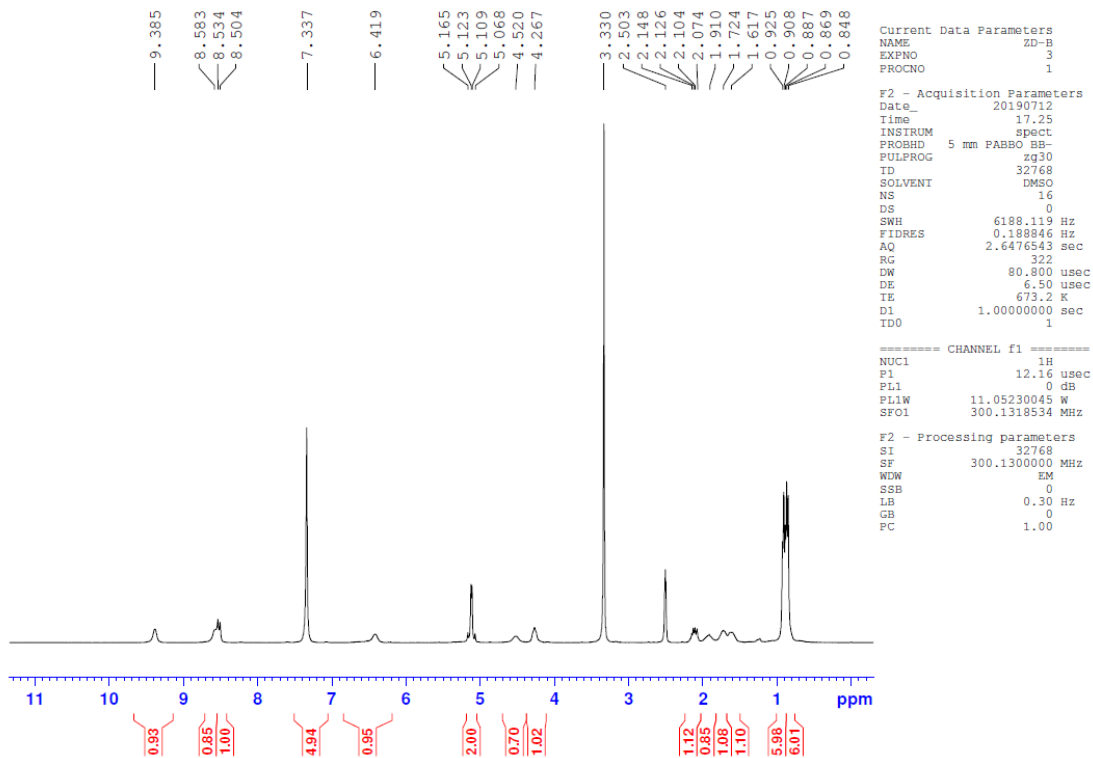


Figure S5 ¹H NMR of ZD-BM.

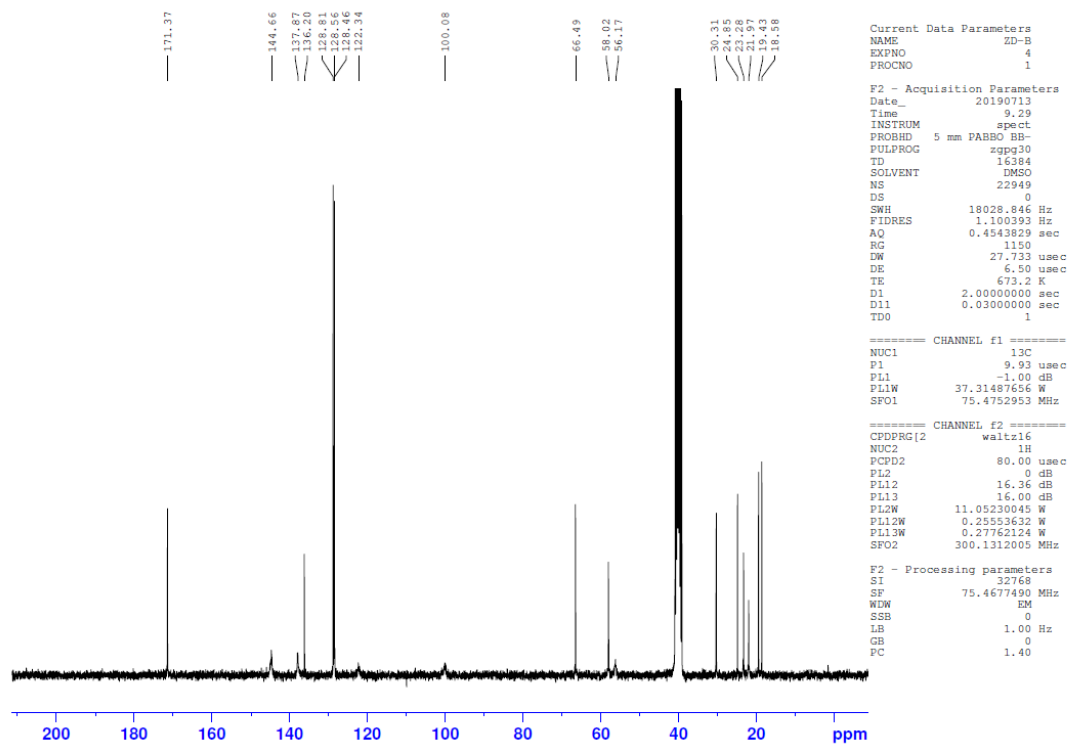


Figure S6 ¹³C NMR of ZD-BM.

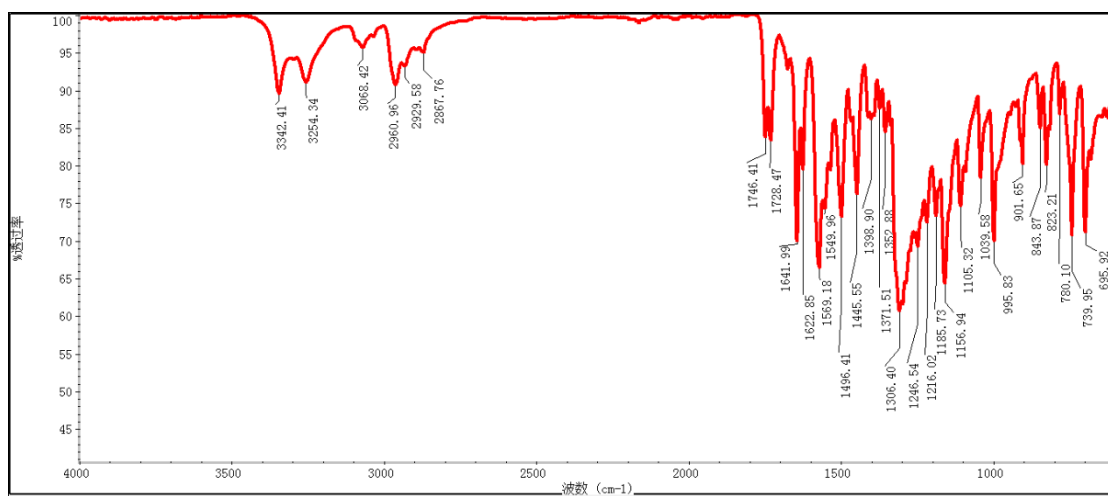


Figure S7 IR of ZD-BM.

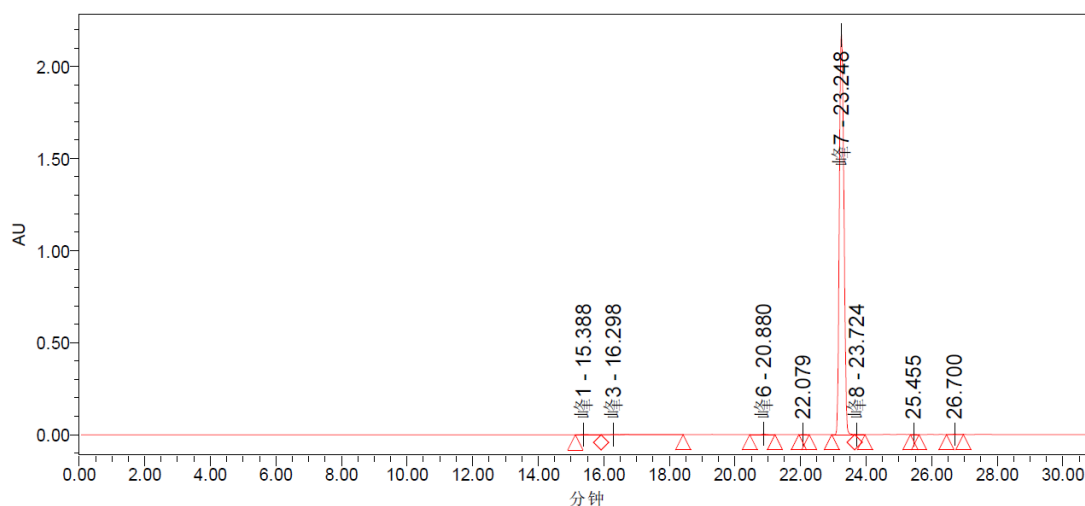


Figure S8 HPLC of ZD-BM.

1.2. Synthesis of ZD-E-1M

1.2.1. Synthesis of benzyl tert-butyl (5-(benzylamino)-5-oxopentane-1,4-diyl)(S)-dicarbamate (1E).

A mixture of Z-Orn(Boc)-OH (3.660 g, 10 mmol) and Benzylamine (1.6 mL, 15 mmol), DCC (2.472 g, 12 mmol), HOBT (1.620 g, 12 mmol), NMM (3.2 mL, 30 mmol) in anhydrous tetrahydrofuran (THF, 100 mL) was stirred at room temperature for 8 h. TLC ($\text{CH}_2\text{Cl}_2:\text{CH}_3\text{OH} = 30:1$, $R_f = 0.38$) was used to monitor the process. The solvent was evaporated in vacuo. The residue was dissolved in 60 mL of EA. And the solution was washed successively with saturated aqueous solution of NaHCO_3 (20 mL \times 3), saturated aqueous solution of NaCl (20 mL \times 3), 5% aqueous solution of KHSO_4 (20 mL \times 3), saturated aqueous solution of NaCl (20 mL \times 3). Then the solution was dried over anhydrous Na_2SO_4 . After filtration, the filtrate was evaporated in vacuo and the crude materials were purified by flash chromatography (column type: SNAP KP-Sil Cartridge; 5% $\text{CH}_3\text{OH}/\text{CH}_2\text{Cl}_2$) to give the 1E (4.490 g, 98.7%) as a white solid. ESI-MS (m/z): 478.3 $[\text{M}+\text{Na}]^+$; ^1H NMR (300 MHz, $\text{DMSO}-d_6$): δ (ppm) = 8.39 (m, 1H), 7.42 (d, $J = 8.0$ Hz, 1H), 7.34 (m, 5H), 7.27 (m, 5H), 6.79 (m, 1H), 5.03 (s, 2H), 4.28 (d, $J = 5.3$ Hz, 2H), 3.99 (m, 1H), 2.89 (t, $J = 5.8$ Hz, 2H), 1.60 (m, 2H), 1.51 (m, 2H), 1.37 (s, 9H).

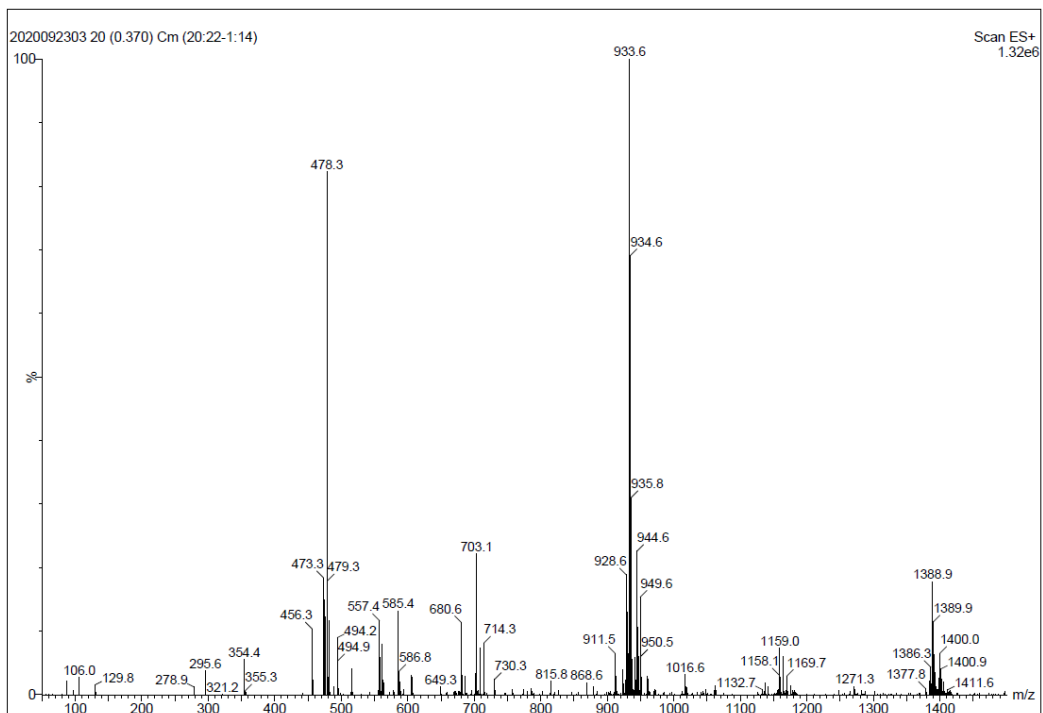


Figure S9 ESI-MS of 1E.

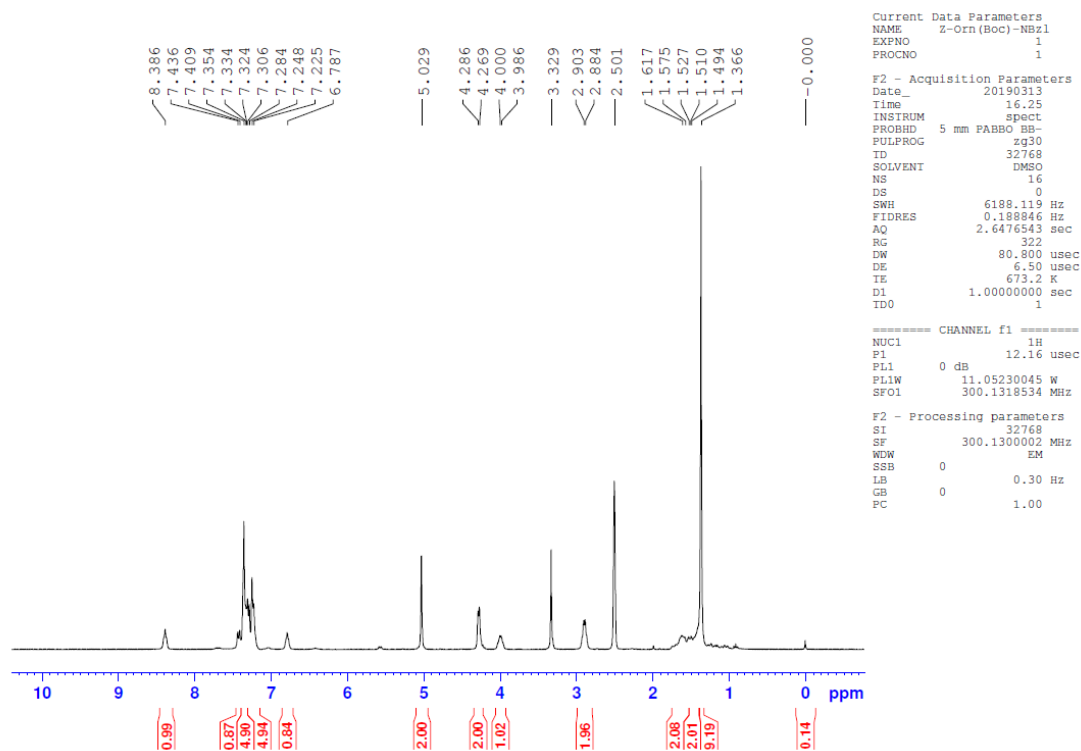


Figure S10 ^1H NMR of 1E.

1.2.2. Synthesis of *tert*-butyl (*S*)-(4-amino-5-(benzylamino)-5-oxopentyl)carbamate (2E).

To the solution of 1E (4.490 g, 9.9 mmol) in CH₃OH (50 mL) was added Pd/C (10%, 0.449 g). The reaction mixture was stirred under H₂ balloon for 4 h at room temperature. After filtration, the filtrate was evaporated in vacuo and provided the 2E (3.988 g, 88.8%) as a white solid. ESI-MS (*m/z*): 322.7 [M+H]⁺.

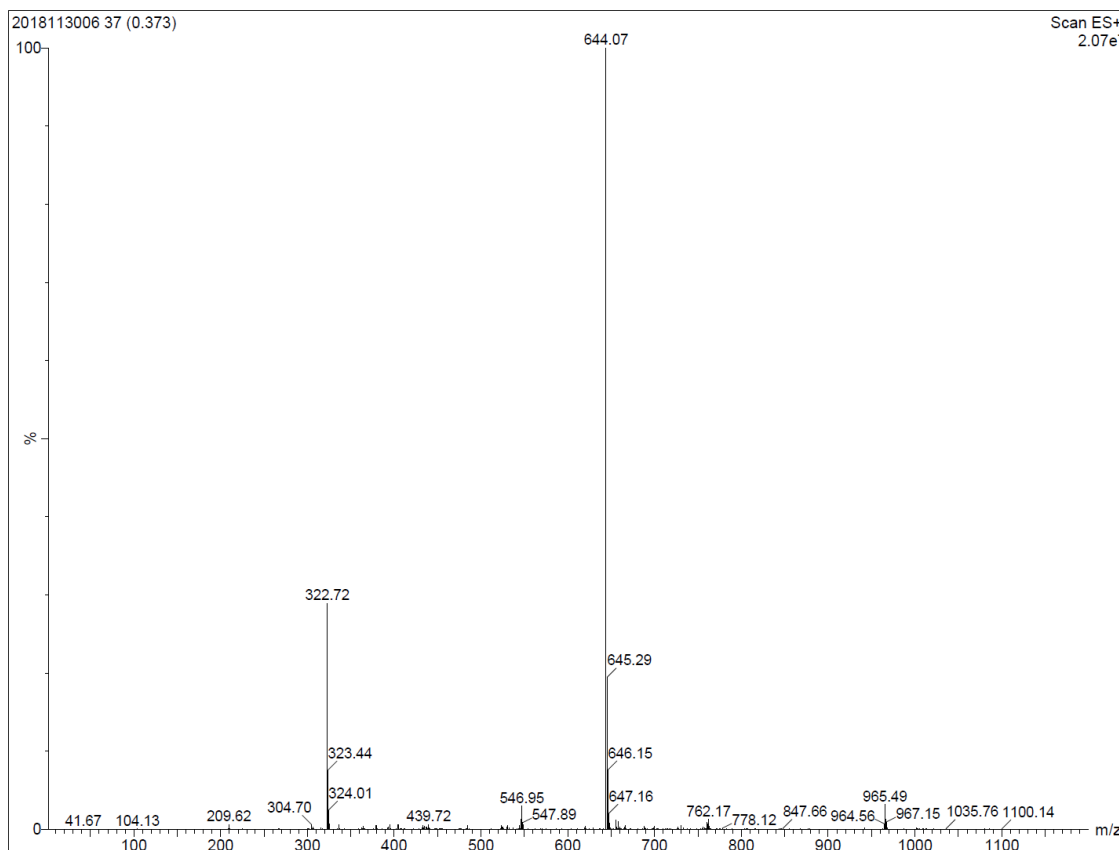


Figure S11 ESI-MS of 2E.

1.2.3. Synthesis of *tert*-butyl (*S*)-(5-(benzylamino)-4-((7-nitrobenzo[*c*][1,2,5]oxadiazol-4-yl)amino)-5-oxopentyl)carbamate (3E).

A mixture of 2E (1.942 g, 6 mmol), 4-chloro-7-nitro-1,2,3-benzoxadiazole (0.998 g, 5 mmol) and DIPEA (5.22 mL, 6 mmol) in 100 mL of methanol anhydrous was stirred at room temperature for 8 h. TLC (PE:EA = 2:1, *R_f* = 0.30) was used to monitor the process. The solvent was evaporated in vacuo and the crude material was purified by flash chromatography (column type: SNAP KP-Sil Cartridge; 35% EA/PE) to provide the 3E (2.028 g, 83.8%) as an orange powder. ESI-MS (*m/z*): 483.4 [M-H]⁻; ¹H NMR (300 MHz, DMSO-*d*₆): δ (ppm) = 9.33 (s, 1H), 8.73 (s, 1H), 8.52 (d, *J* = 8.8 Hz, 1H), 7.26 (m, 5H), 6.81 (t, *J* = 5.1 Hz, 1H), 6.33 (s, 1H), 4.37 (m, 1H), 4.32 (t, *J* = 4.7 Hz, 2H), 2.96 (t, *J* = 6.1 Hz, 2H), 1.96 (m, 2H),

1.53 (m, $J = 7.0$ Hz, 2H), 1.35 (s, 9H); ^{13}C NMR (75 MHz, $\text{DMSO-}d_6$): δ (ppm) = 170.5, 156.1, 156.0, 144.8, 144.5, 139.4, 138.0, 128.7, 127.7, 127.3, 122.3, 100.3, 77.9, 57.9, 42.8, 42.7, 39.9, 28.7, 27.7.

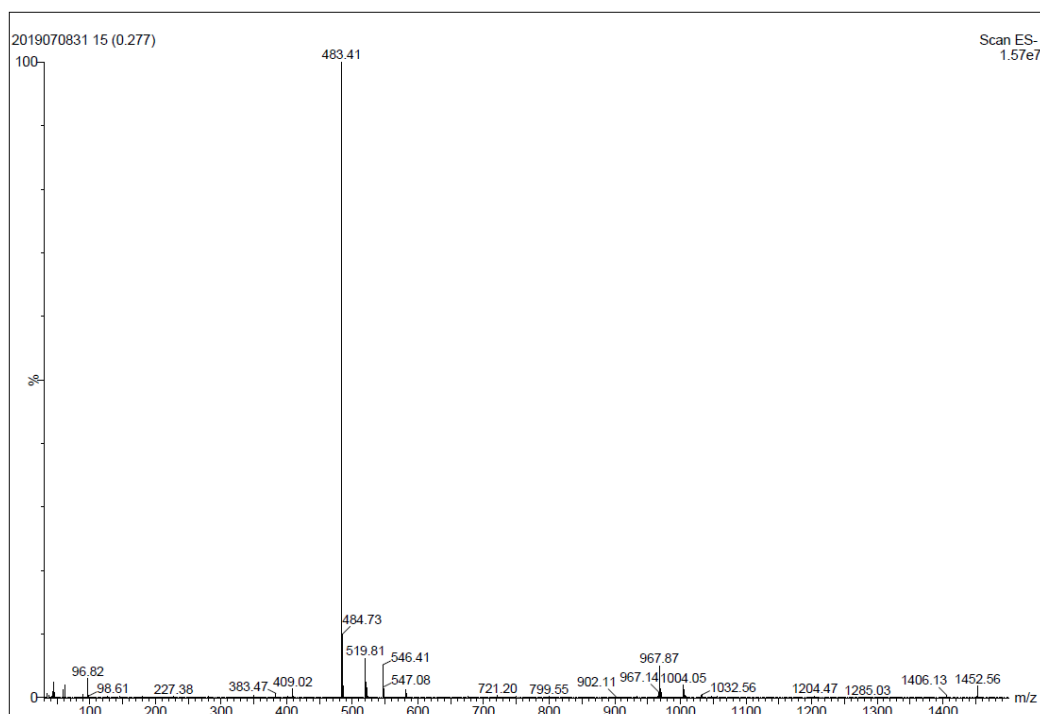


Figure S12 ESI-MS of 3E.

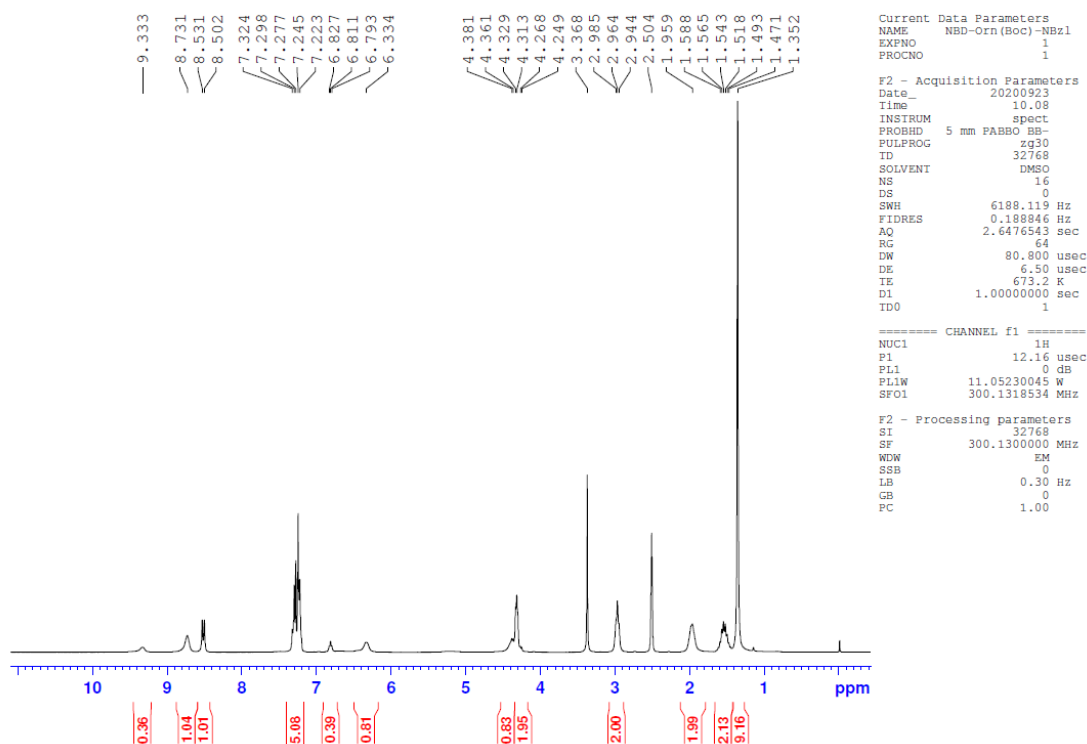


Figure S13 ^1H NMR of 3E.

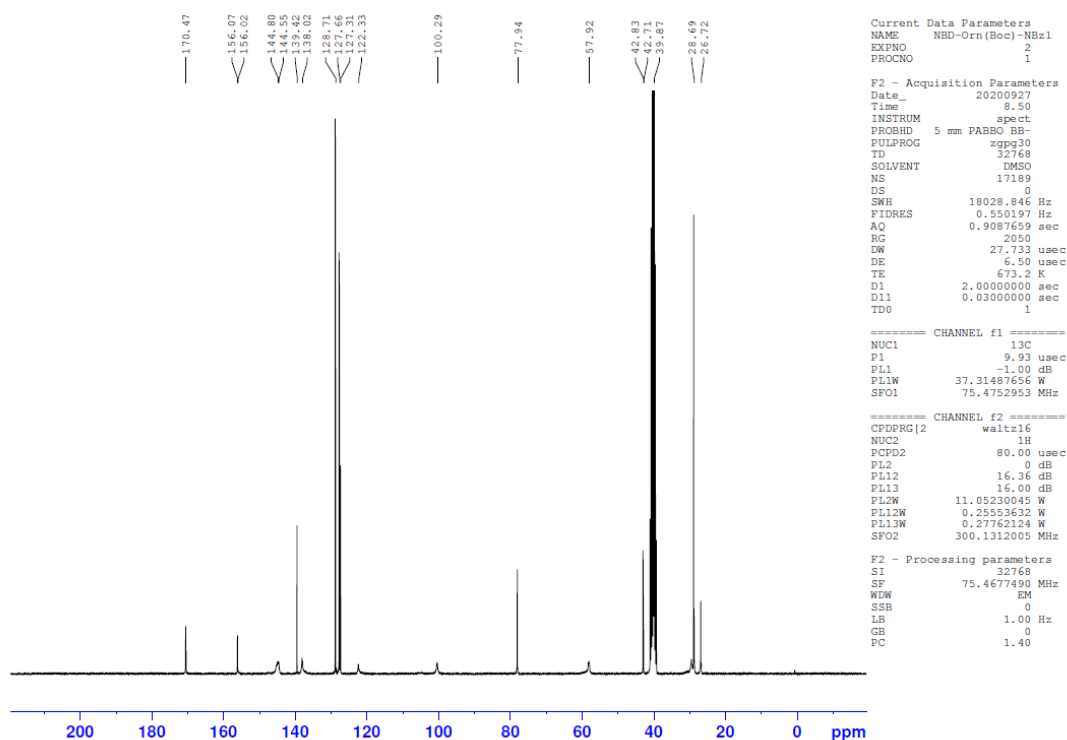


Figure S14 ^{13}C NMR of 3E.

1.2.4. *Synthesis* of
(*S*)-5-amino-*N*-benzyl-2-((7-nitrobenzo[*c*][1,2,5]oxadiazol-4-yl)amino)pentanamide (ZD-E).

A mixture of 3E (2.028 g, 5.5 mmol) and 2 mol/L HCl/EA (20 mL) was stirred with at 0 °C for 2 h. The solvent was evaporated in vacuo with dried EA (10 mL × 3) and diethyl ether (10 mL × 1) to give the intermediate ZD-E (1.762 g, 96.1%) as an orange solid, m.p. 128.5–130.1 °C; = -26.4, (C 0.1, CH₃OH); FT-MS (*m/z*): 385.1619 [M+H]⁺; ^1H NMR (300 MHz, DMSO-*d*₆): δ (ppm) = 9.41 (s, 1H), 9.00 (t, *J* = 5.2 Hz, 1H), 8.54 (d, *J* = 8.8 Hz, 1H), 7.28 (m, 5H), 6.40 (s, 1H), 4.52 (m, 1H), 4.32 (d, *J* = 5.5 Hz, 2H), 2.82 (m, 2H), 2.04 (m, 2H), 1.91 (s, 1H), 1.72 (m, 2H); ^{13}C NMR (75 MHz, DMSO-*d*₆): δ (ppm) = 170.4, 170.2, 139.4, 139.4, 128.7, 127.6, 127.3, 42.8, 42.7, 38.5, 38.5, 33.8, 24.2.

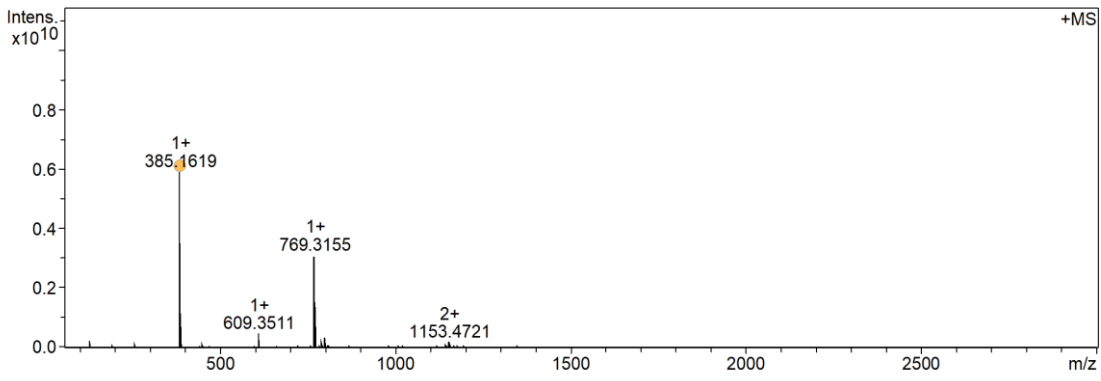


Figure S15 FT-MS of ZD-E.

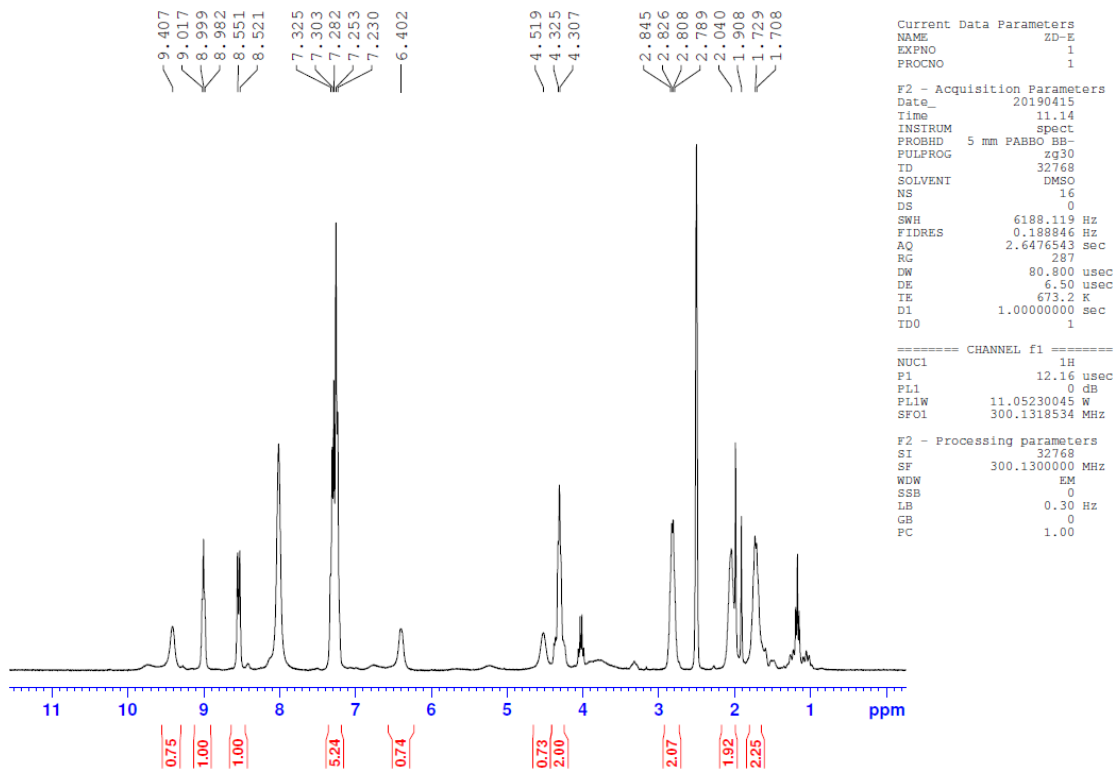


Figure S16 ¹H NMR of ZD-E.

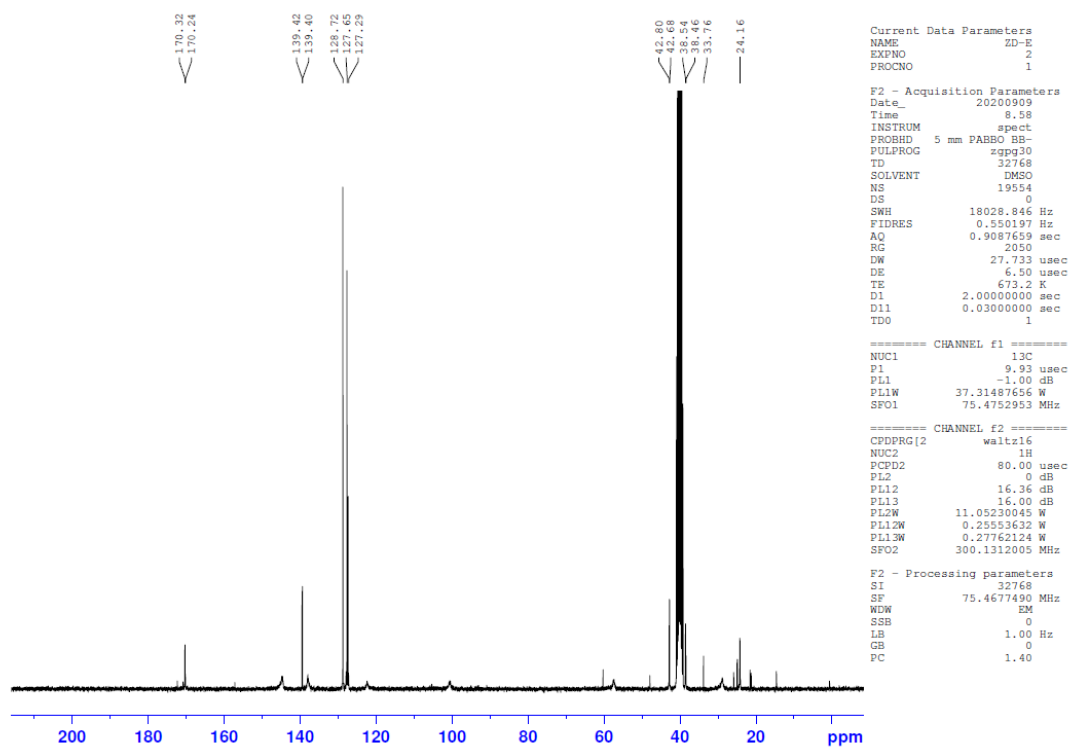


Figure S17 ¹³C NMR of ZD-E.

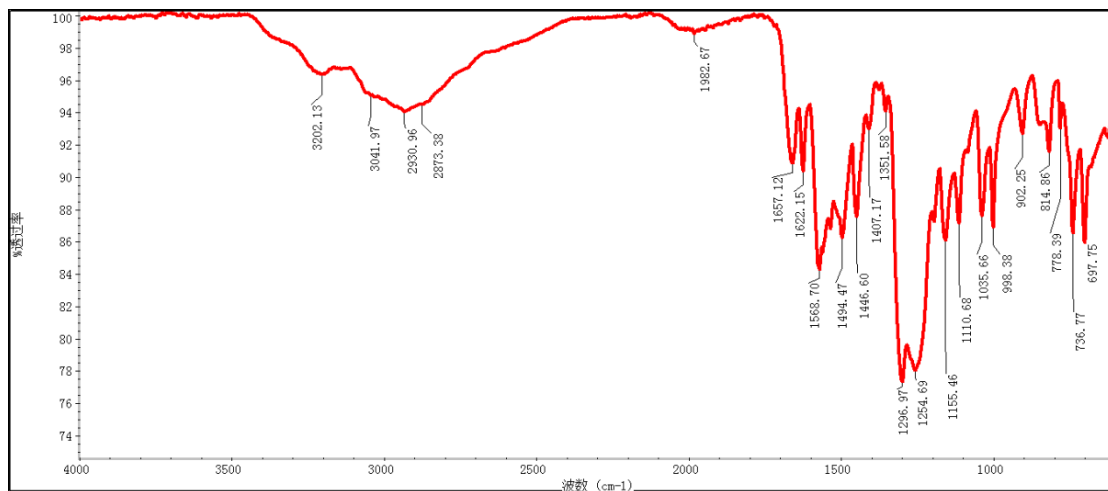


Figure S18 IR of ZD-E.

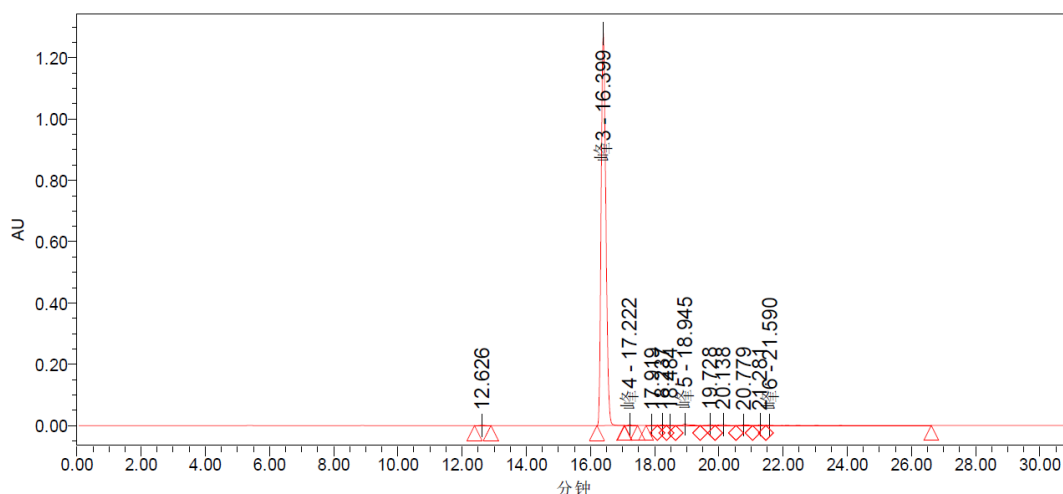


Figure S19 HPLC of ZD-E.

1.2.5. *Synthesis* of *(S)-N-benzyl-5-(2-chloroacetimidamido)-2-((7-nitrobenzo[*c*][1,2,5]oxadiazol-4-yl)amino)pentanamide (ZD-E-1M)*.

A mixture of ZD-E (420 mg, 1 mmol), ethyl 2-chloroacetimidate (705 mg, 5 mmol), DIPEA (1.1 mL, 1.2 mmol) in methanol anhydrous was stirred at room temperature for 8h without light. TLC (EA:H₂O:HAc = 6:1:1, R_f = 0.38) was used to monitor the process. The solvent was evaporated in vacuo and the crude material was purified by flash chromatography (column type: SNAP Ultra C18 Cartridge; 40% CH₃OH/H₂O) to give the target compound ZD-E-1M (210 mg, 50.0%) as an orange powder, m.p. $[\alpha]_D^{25}$ 88.2–90.0 °C; = –14.0, (C 0.1, CH₃OH); FT-MS (*m/z*): 494.1116 [M+Cl][–]; ¹H NMR (300 MHz, DMSO-*d*₆): δ (ppm) = 9.94 (s, 1H), 9.52 (s, 1H), 9.35 (s, 1H), 9.09 (s, 1H), 8.79 (s, 1H), 8.56 (d, *J* = 8.7 Hz, 1H), 7.26 (m, 5H), 6.36 (s, 1H), 4.40 (m, 1H), 4.36 (s, 2H), 4.31 (m, 2H), 3.29 (m, 2H), 2.03 (m, 2H), 1.68 (m, 2H); ¹³C NMR (75 MHz, DMSO-*d*₆): δ (ppm) = 170.2, 167.3, 162.8, 158.9, 158.4, 139.4, 128.7, 127.7, 127.3, 118.2, 114.4, 58.6, 42.8, 42.2, 41.4, 24.7, 24.3.

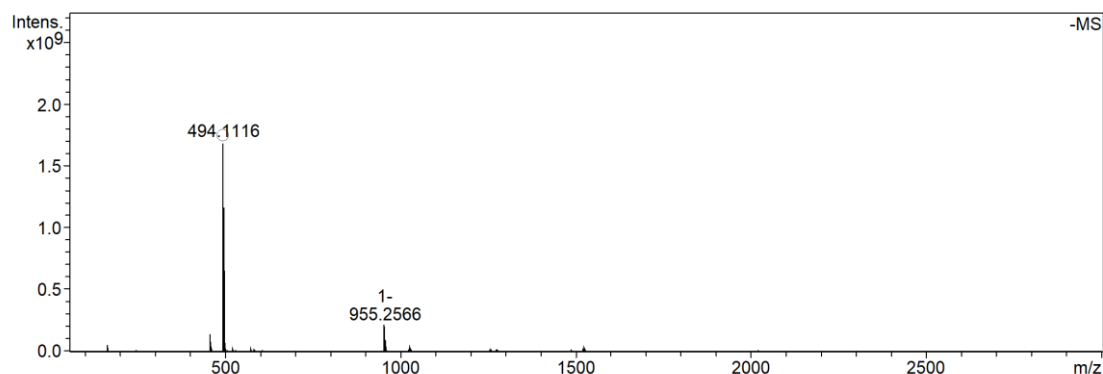


Figure S20 FT-MS of ZD-E-1M.

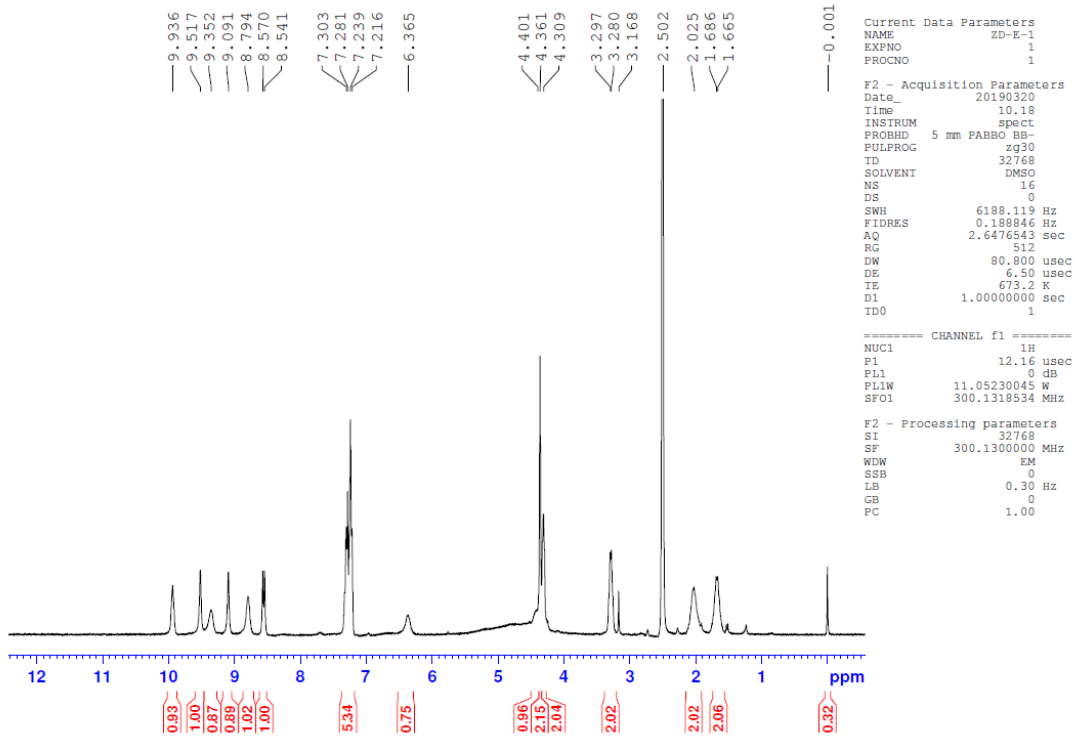


Figure S21 ¹H NMR of ZD-E-1M.

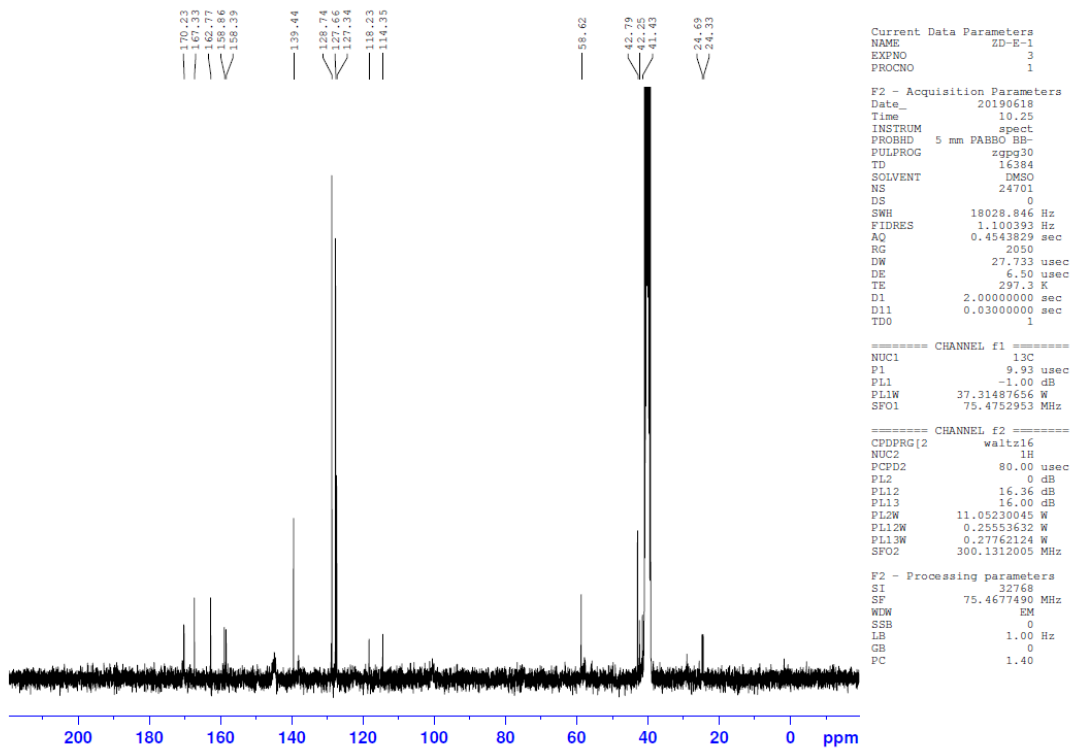


Figure S22 ¹³C NMR of ZD-E-1M.

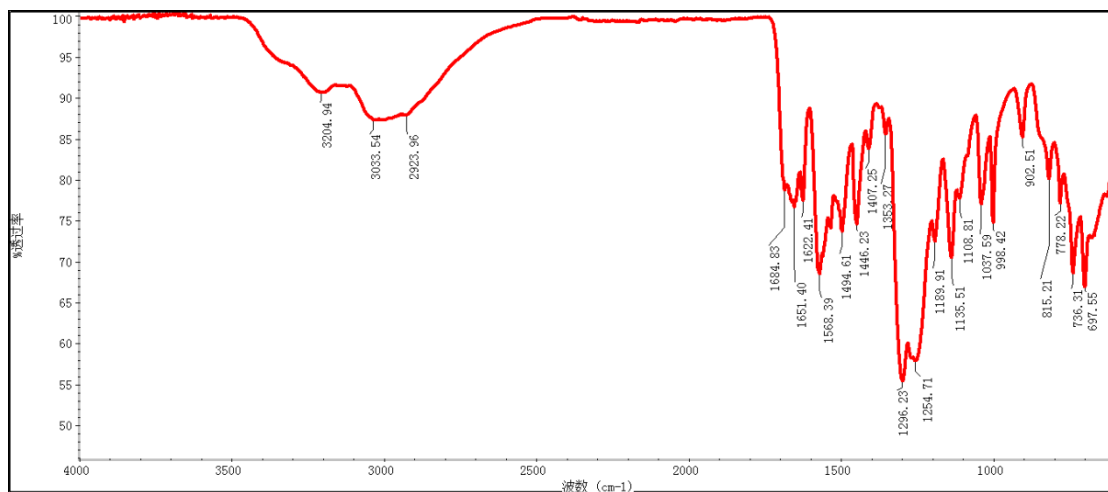


Figure S23 IR of ZD-E-1M.

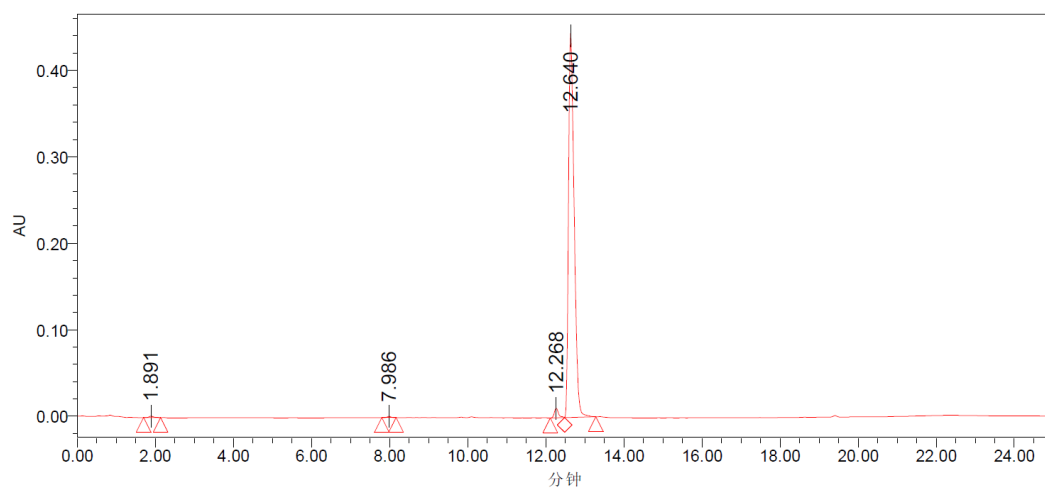


Figure S24 HPLC of ZD-E-1M.

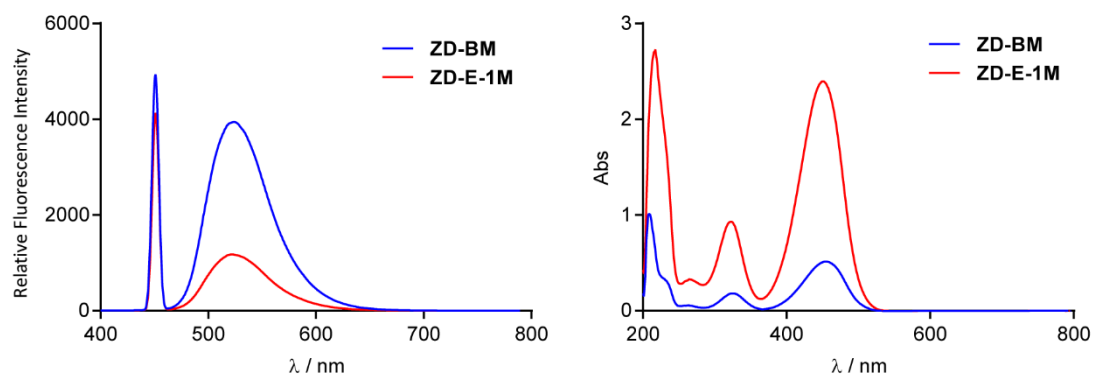


Figure S25 UV and fluorescence spectrum of ZD-BM and ZD-E-1M.

2. Results

Table S1 Molecular docking of compounds toward active site of PAD4 enzyme.

Compounds	PAD4-CDOCKER Energy (Kcal/mol)
YW3-56	43.91
ZD-E-1M	48.755
ZD-BM	47.628

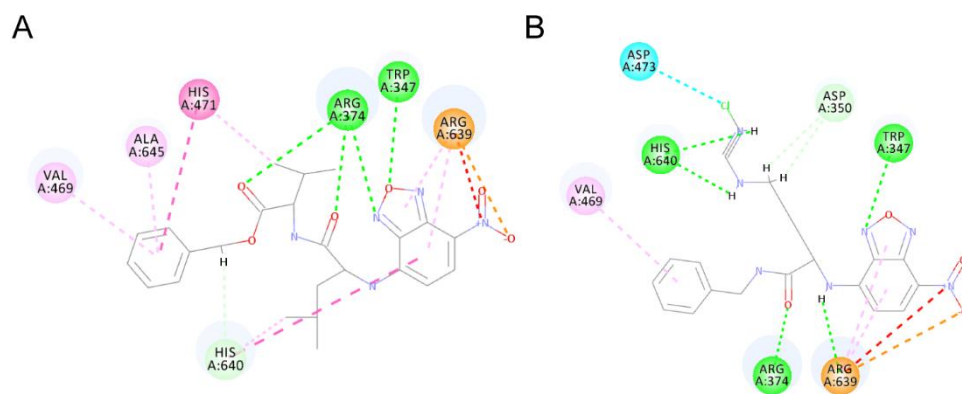


Figure S26 2D schematic diagram of docking model of (A) ZD-E-1M and (B) ZD-BM with PAD4.

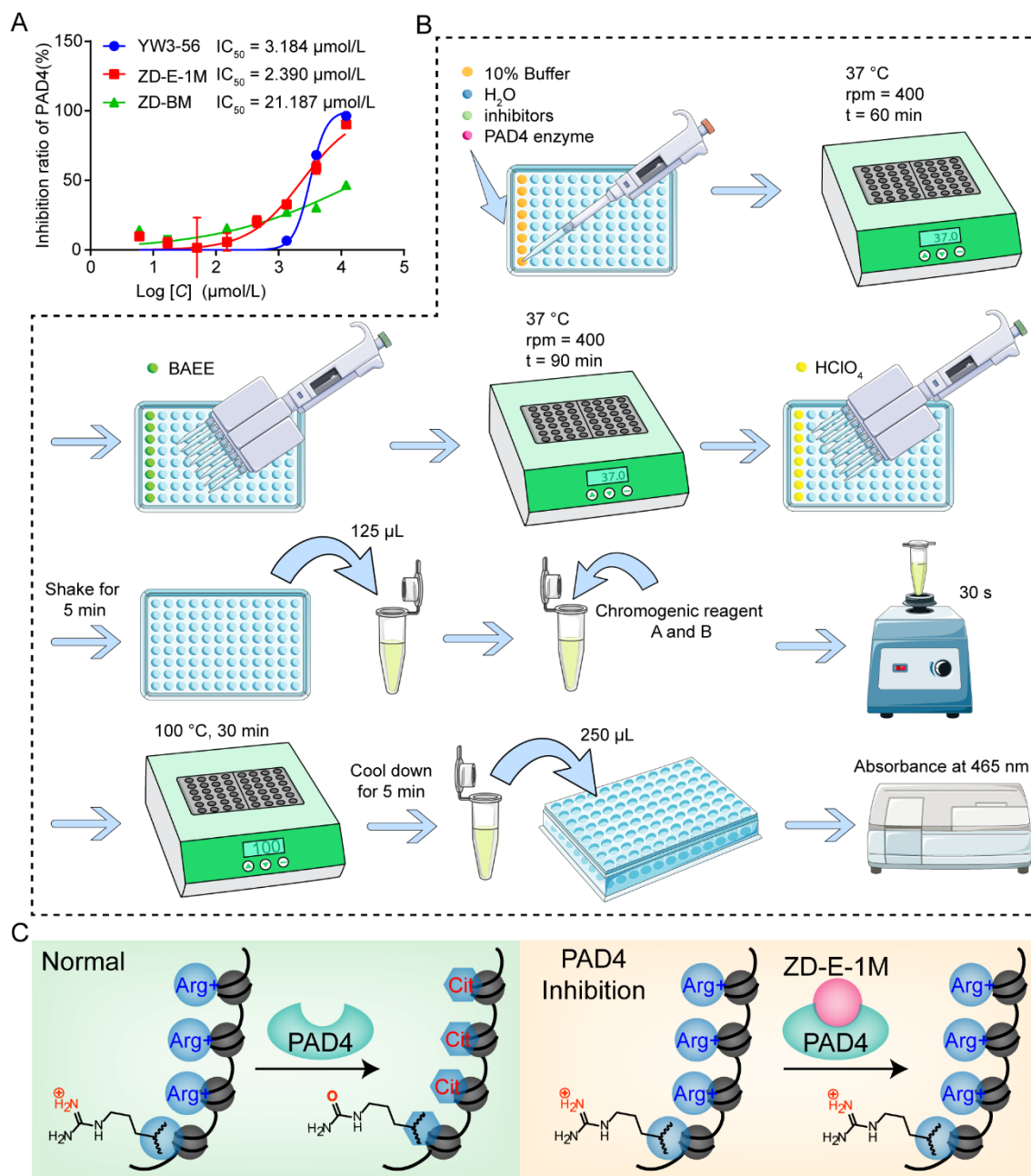


Figure S27 PAD4 inhibition activity assessed by a colorimetric method. (A) PAD4 inhibition ratio of YW3-56, ZD-BM and ZD-E-1M. (B) The experimental workflow of PAD4 inhibition determination. (C) Mechanism of ZD-E-1M inhibiting PAD4. Data are presented as mean \pm SD ($n = 3$).

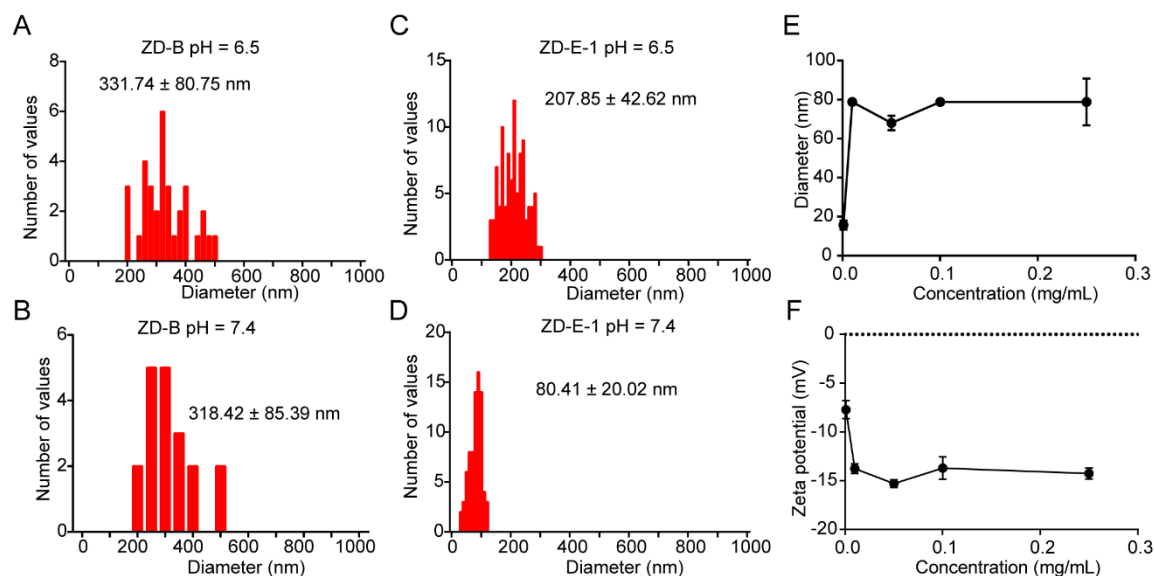


Figure S28 Nano self-assembly characterization. (A–D) Size distribution of ZD-B and ZD-E-1 at pH 6.5 and pH 7.4 in TEM photos analyzed by ImageJ. (E–F) Size and zeta potential changes with concentration of ZD-E-1. Data are presented as mean \pm SD ($n = 3$).

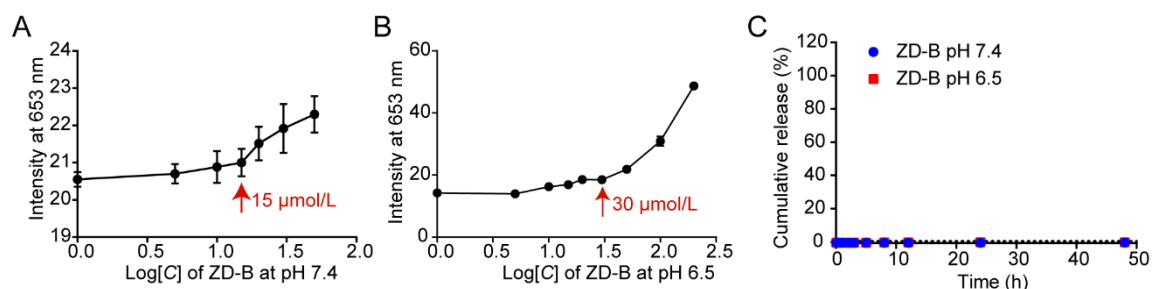


Figure S29 Nano self-assembly properties of ZD-B. (A–B) The critical aggregation concentration (CAC) at pH 7.4 and pH 6.5. (C) Drug release curve at pH 7.4 and pH 6.5. Data are presented as mean \pm SD ($n = 3$).

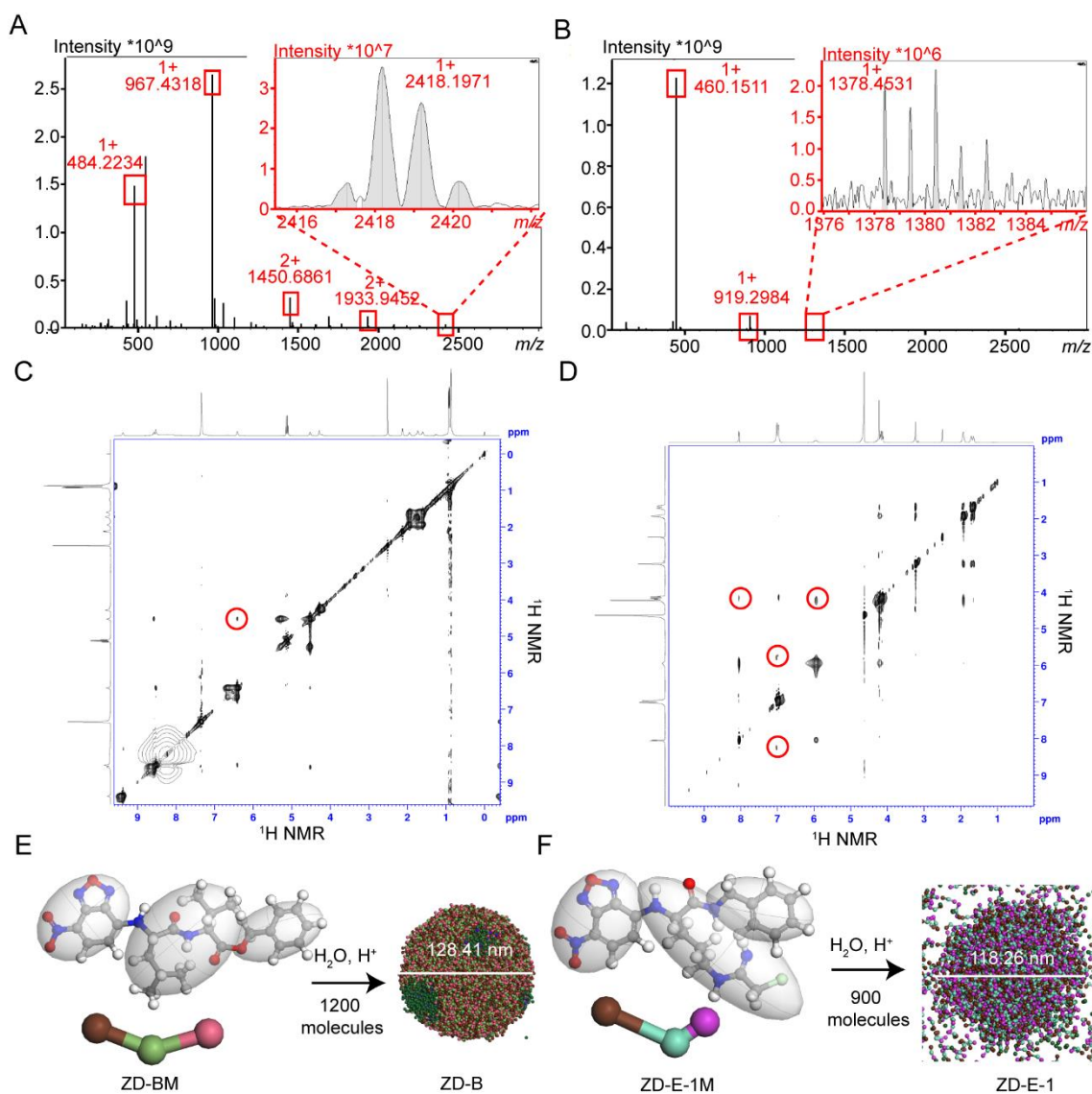


Figure S30 FTMS spectra and NOSEY 2D NMR in acid solvent. (A–B) FTMS spectra of ZD-B and ZD-E-1 at pH 6.5. (C–D) NOSEY 2D NMR of ZD-B and ZD-E-1 at pH 6.5. (E–F) Molecular dynamics simulation of ZD-B and ZD-E-1 in self-assembled nano-units in acidic solution.

Table S2 IC₅₀ values of compounds determined after 48 h incubation

Drug	IC ₅₀ values (X ± SD μmol/L)					
	HL7702	4T1	MDA-MB-231	S180	A549	LLC
YW3-56	7.5 ± 2.7	11.9 ± 0.7	7.0 ± 0.5	8.4 ± 1.8	9.7 ± 4.2	6.1 ± 1.6
ZD-B	> 100	94.7 ± 5.7	105.7 ± 1.3	74.4 ± 10.1	> 100	96.5 ± 6.9
ZD-E-1	67.2 ± 15.0	7.9 ± 0.9	11.4 ± 1.6	24.6 ± 1.7	28.8 ± 1.1	26.1 ± 2.6

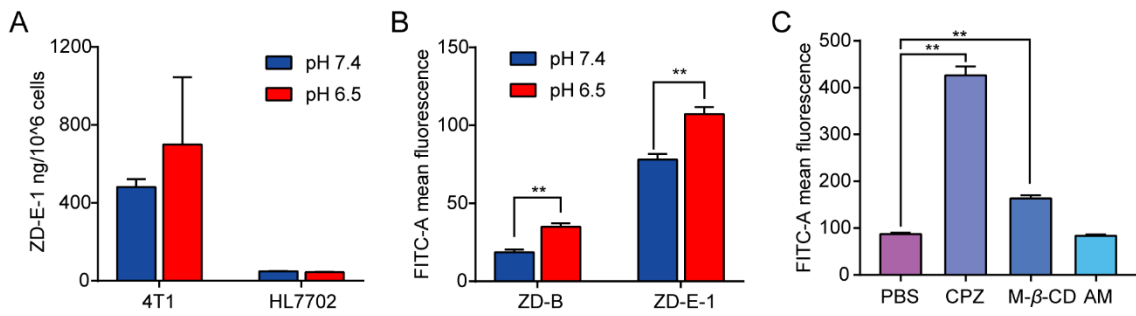


Figure S31 Uptake behavior and uptake pathway. (A) The uptake of ZD-E-1 was measured by HPLC-MS (SCIEX) on 4T1 and HL7702 cells at different pH values for 48 h. (B) Flow cytometry (BD) measured the uptake of ZD-B and ZD-E-1 by 4T1 cells at different pH values for 48 h. (C) Flow cytometry (BD) measured the uptake pathway of ZD-E-1 by 4T1 cells. Data are presented as mean \pm SD ($n = 3$). * $P < 0.05$ and ** $P < 0.01$.

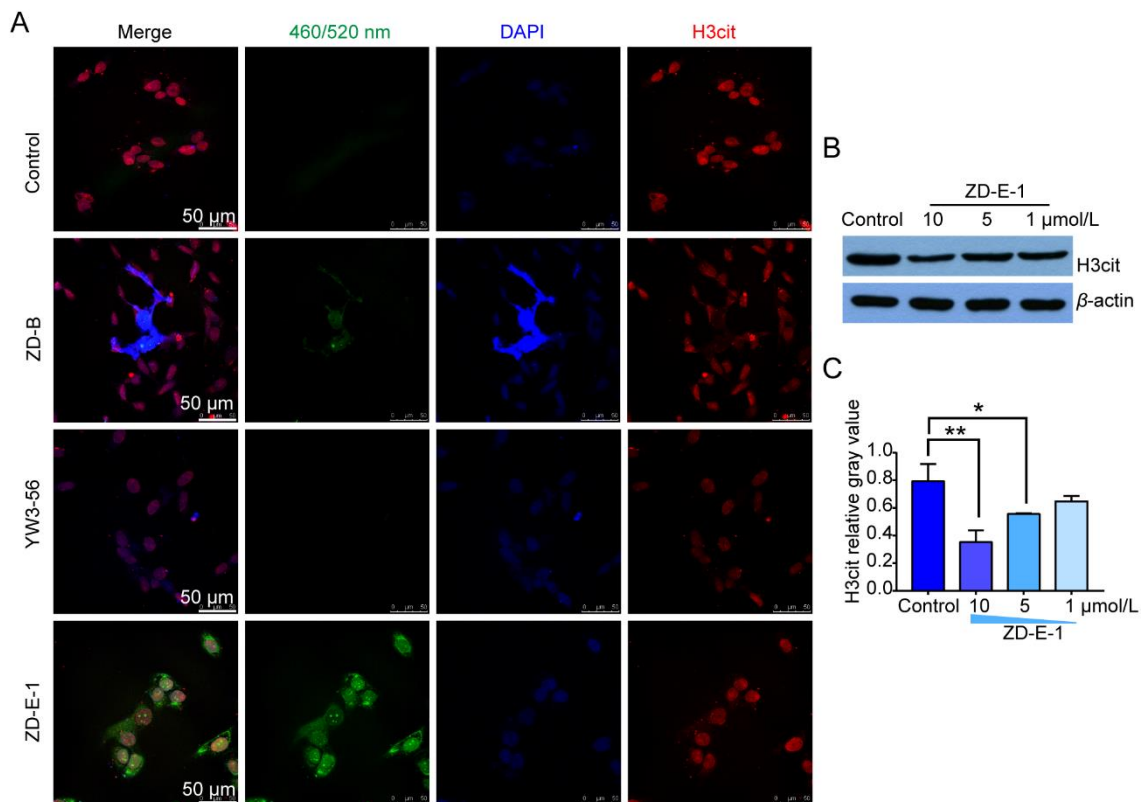


Figure S32 (A) The levels of H3cit and subcellular colocalization of ZD-E-1 and H3cit in 4T1 cells determined by CLSM (Leica). (B–C) Protein expression in 4T1 cells treated with ZD-E-1 (10, 5 and 1 $\mu\text{mol/L}$) evaluated by immunoblotting and gray value analysis. Data are presented as mean \pm SD ($n = 3$). * $P < 0.05$ and ** $P < 0.01$.

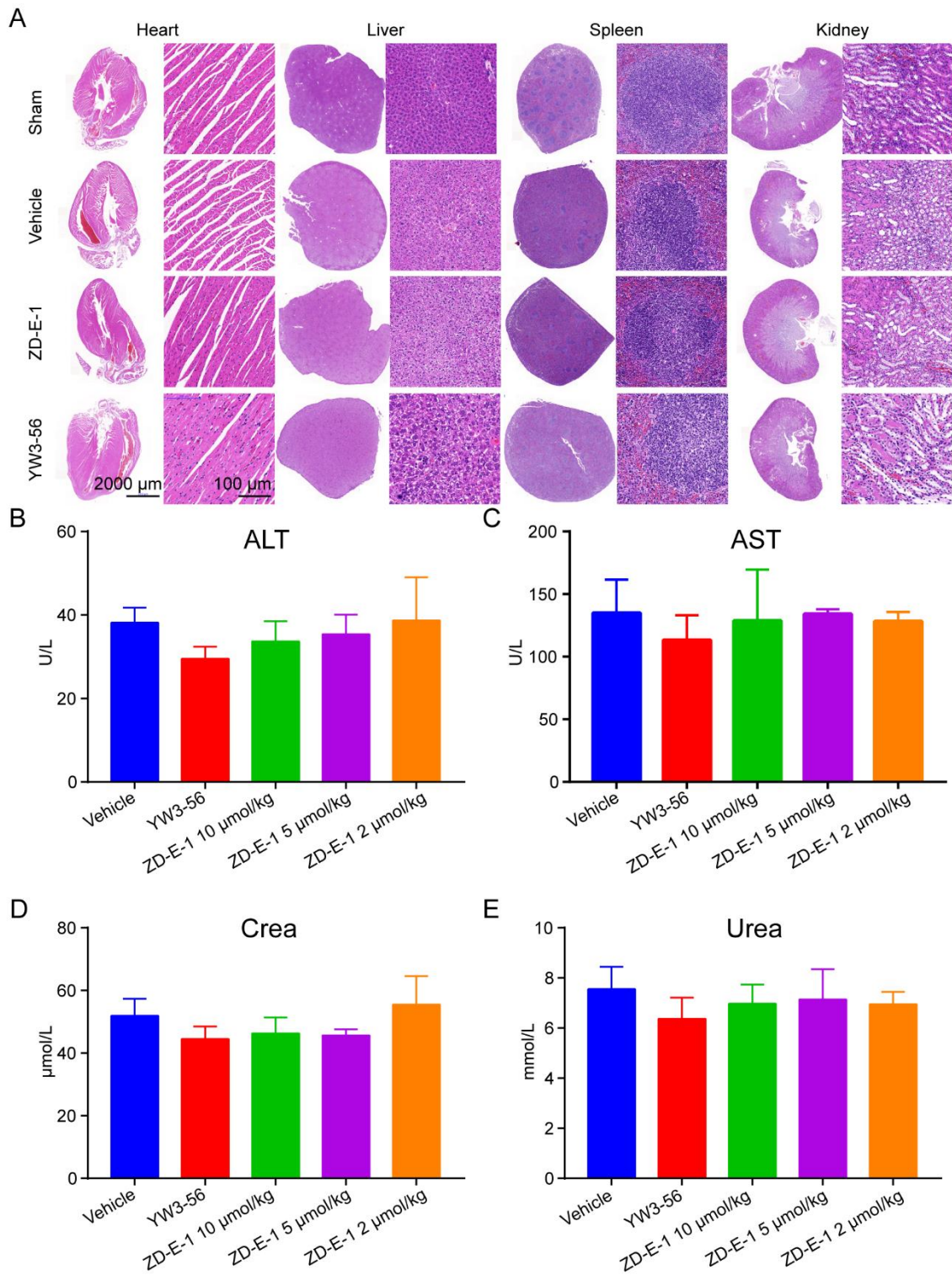


Figure S33 The nanotoxicity of ZD-E-1 on 4T1 orthotopic tumor-bearing mice. (A) Histological analysis of main organs by HE staining; (B–E) ALT, AST, Crea, and urea levels in serum. Data are presented as mean \pm SD ($n = 3$).

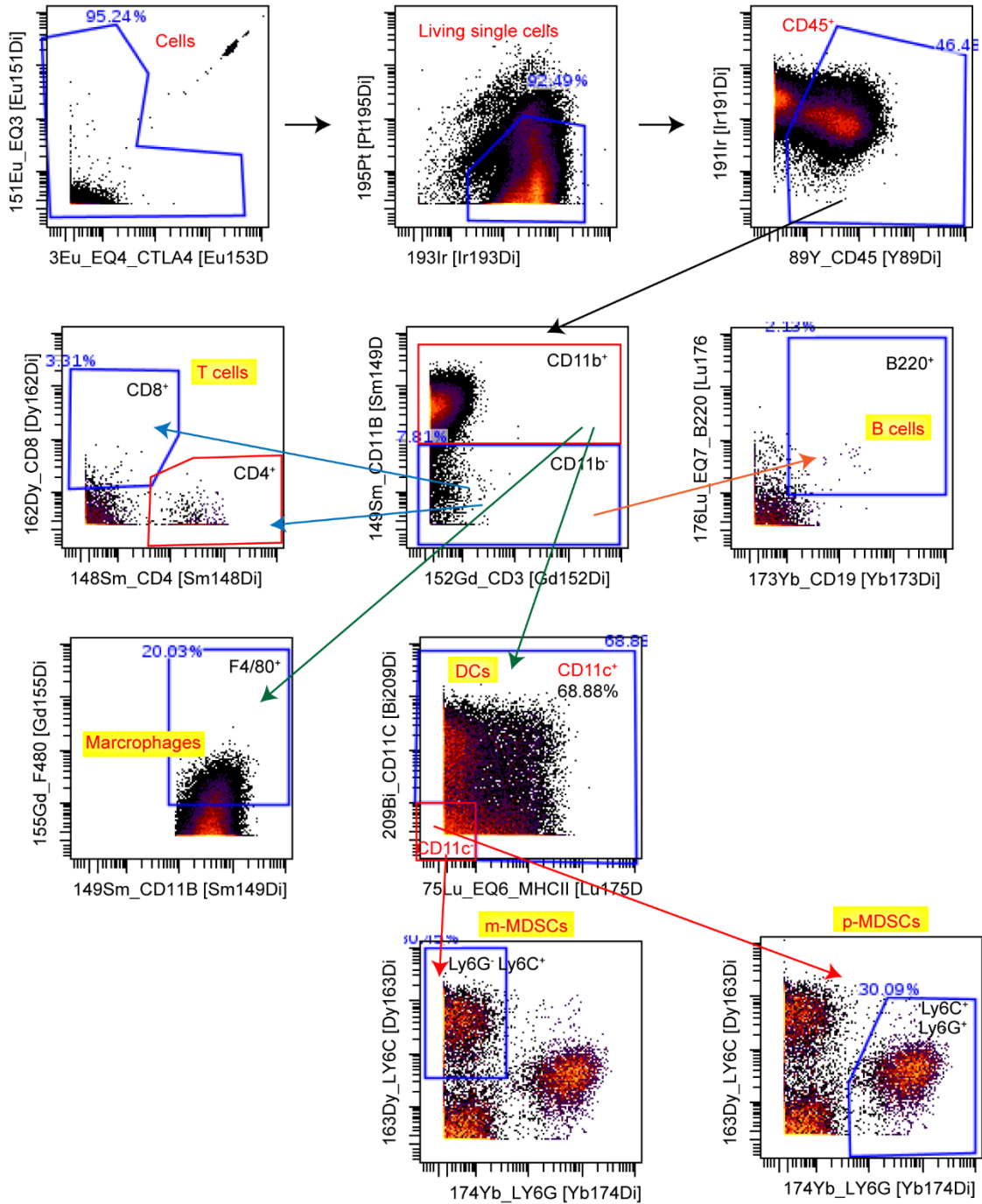


Figure S34 Gating hierarchy plots.

Table S3 Penal of mass cytometry.

Antibody	Metal	Clone	Company	Antibody	Metal	Clone	Company
CD45	89	30-F11	Fluidigm	CCR7	159	4B12	biolegend
CXCR5	106	L138D7	biolegend	CD62L	160	MEL-14	biolegend
TNF α	141	MP6-XT22	Fluidigm	INOS	161	CXNFT	Fluidigm
NK1.1	142	S17016D	biolegend	CD8	162	53-6.7	biolegend

TCRgd	143	GL3	biolegend	LY6C	163	HK1.4	biolegend
PD1	144	RMP1-30	biolegend	CD49B	164		Fluidigm
CD69	145	H1.2F3	biolegend	FOXP3	165	MF-14	biolegend
CD206	146	QA17A35	biolegend	GranzymeB	167		RD
ARG-1	147	094E6/ARG1	biolegend	CCR4	168	2G12	biolegend
CD4	148	RM4-4	biolegend	CD205	169	NLDC-145	biolegend
CD11b	149	M1/70	biolegend	CXCR3	170	S18001A	biolegend
CD25	150	3C7	Fluidigm	CD44	171	IM7	Fluidigm
CD3	152	145-2C11	biolegend	CD86	172	GL-1	biolegend
CTLA4	153	UC10-4B9	biolegend	CD19	173	6D5	biolegend
KI67	154	16A8	biolegend	LY6G	174	RB6-8C5	biolegend
F4/80	155	BM8	biolegend	MHCII	175		abcam
CD127	156	SB-199	biolegend	B220	176	RA3-6B2	biolegend
LAG3	158	C9B7W	biolegend	CD11C	209	N418	Fluidigm

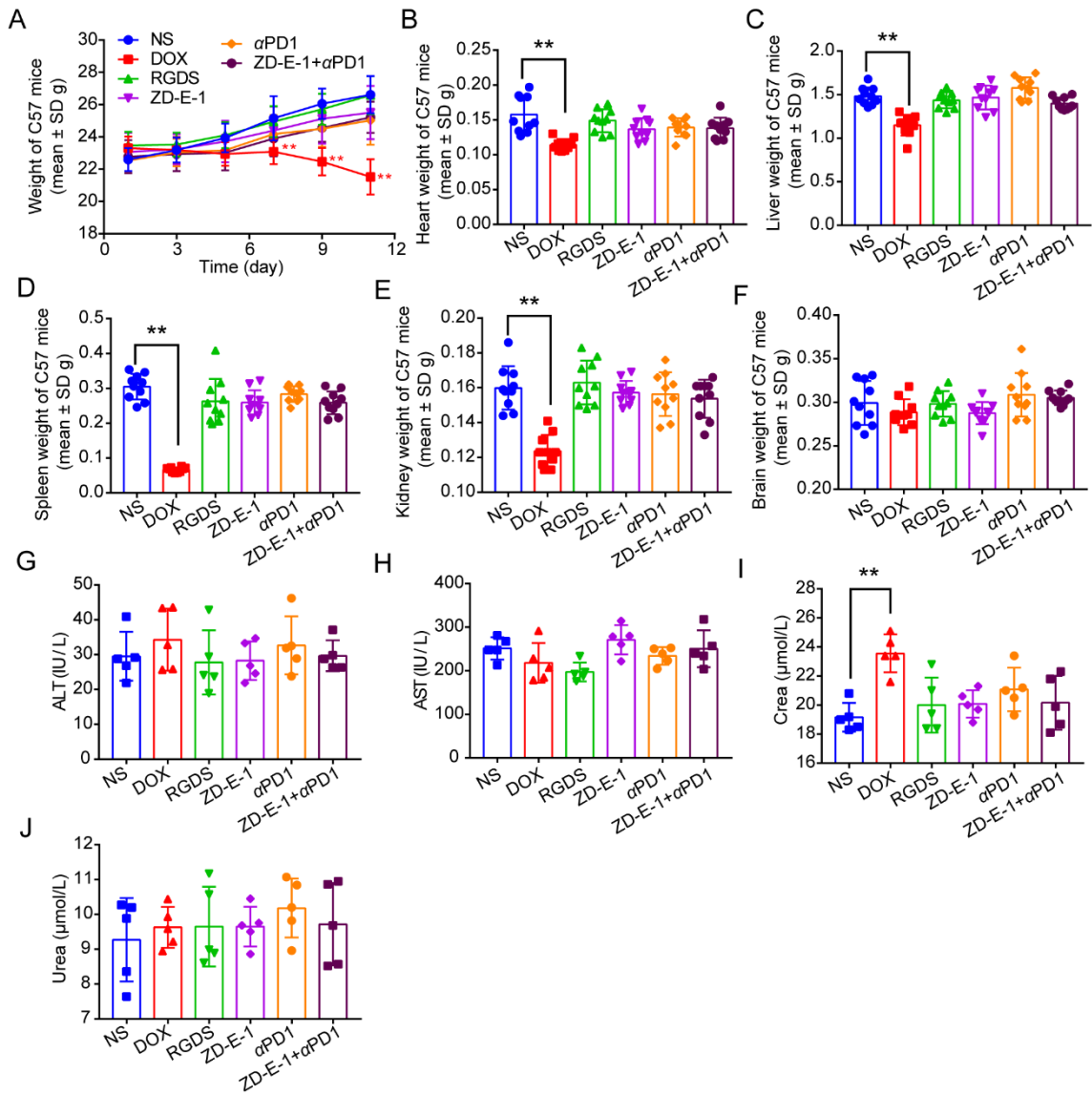


Figure S35 The nanotoxicity of ZD-E-1 on LLC tumor-bearing mice. (A) Body weight of LLC tumor-bearing mice. (B–F) Main organs weight of LLC tumor-bearing mice. (G–J) ALT, AST, Crea, and urea levels in serum. Data are presented as mean ± SD ($n = 6$). ** $P < 0.01$.

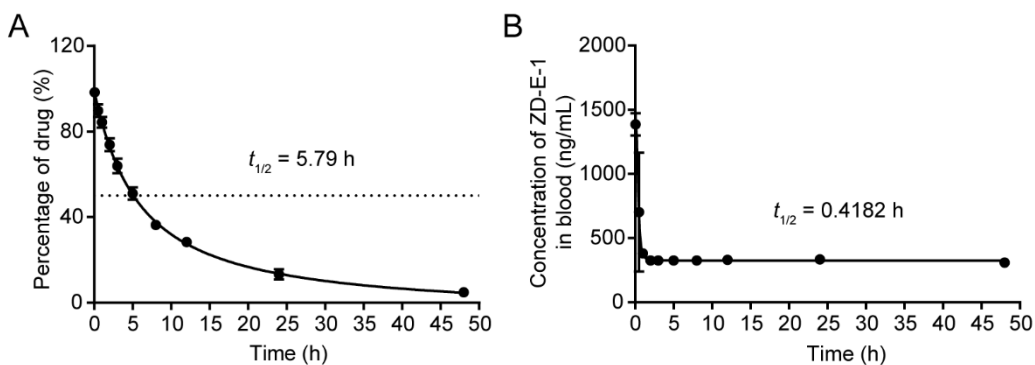


Figure S36 The serum stability (A) and pharmacokinetics (B) determined by HPLC-MS (SCIEX). Data are presented as mean ± SD ($n = 3$).

3. Materials and methods

3.1. Materials and reagents

Methanol anhydrous, ethanol, CH₂Cl₂, CH₃OH, PE, EA, diethyl ether, NaOH, KHSO₄, NaCl, Na₂SO₄, DMF were purchased from Beijing Chemical Reagent Company (Beijing, China). L-Orn(Boc)-OBzl (BeiJing BoMaiJie Technology Co., Ltd., Beijing, China), RPMI 1640 medium (Gibco, 31800-022, Carlsbad, CA, USA), DMEM medium (Gibco, 12100-046, Carlsbad, CA, USA), FBS (Corning, 35-076-CV, Corning, NY, USA), Penicillin G Sodium salt (100 U/mL) (Solarbio, P8420, Beijing, China), Streptomycin Sulfate (Solarbio, S8290, Beijing, China), MTT ((3-(4,5-dimethylthiazol-2-yl)2,5-diphenyl-tetrazolium bromide) (Aladdin, CAS:298-93-1, Toronto, Canada), 0.25% trypsin (Hyclone, KGY0012, Logan, UT, USA), DOX (Sigma-Aldrich, 23214-92-8, Darmstadt, Germany), DMSO (Sigma-Aldrich, 67-68-5, Darmstadt, Germany), PBS (KeyGEN BioTECH, KGB5001, Nanjing, China), Cell lysis buffer for Western and IP (Beyotime, P0013, Beijing, China), 4% paraformaldehyde solution (Solarbio, P1110, Beijing, China), T25 cell culture flask (Corning, 430639, Corning, New York, USA), BCA protein assay reagent (Beyotime, P0012, Beijing, China), BSA (Amresco, A7030, Solon, OH, USA), EDTA (pH 9.0) antigen repair solution (Genepool, GPB1837, Beijing, China), DAPI (Beyotime, C1006, Beijing, China), ECL chromogenic solution (GenePool, GPP1824, Beijing, China), Goat anti-Rabbit IgG H&G (Biotin) (Abcam, ab6720, London, England), Streptavidin (HRP) (Abcam, ab7403, London, England), DAB Kit (20X) (Genepool, GPP1823, Beijing, China), LC3B antibody (CST, 2775, Danvers, MA, USA), SQSTM1/p62 antibody (CST, 5114, Danvers, MA, USA), H3cit antibody (Abcam, ab5103, London, England), Goat anti-Mouse IgG, HRP (Abcam, ab6789, London, England), Goat anti-Rabbit IgG, HRP (Abcam, ab6721, London, England), and anti- β -actin antibody (Abcam, ab6276, London, England), A23187 (Cayman, 52665-69-7, Ann Arbor, MI, USA), Chlorpromazine (Aladdin, 50-53-3, Shanghai, China), methyl- β -cyclodextrin (Aladdin, 128446-36-6, Shanghai, China), and Amiloride hydrochloride (Aladdin, 2016-88-8, Shanghai, China).

S180 (mouse sarcoma S180 cells), A549 (human lung carcinoma cells), LLC (mouse Lewis lung cancer cells), 4T1 (human breast carcinoma cells), MDA-MB-231 (human breast carcinoma cells), HL7702 (normal human embryonic hepatocytes) were purchased from KeyGEN BioTECH. S180 and A549 cancer cells were maintained in RPMI 1640 medium supplemented with 10% FBS, LLC, 4T1, MDA-MB-231 and HL7702 cells were cultured in DMEM medium supplemented with 10% FBS.

3.2. Methods

3.2.1. Molecular docking

The 3D structures of target compounds were built by a 3D-sketcher module and energy was minimized in Discovery Studio 4.0. The crystal structure of PAD4 (PDB ID: 1WDA) was obtained from the Protein Data Bank (PDB). Before docking, the water molecules were removed and the protein was cleaned. The hydrogen atoms were added to the protein, which was then defined as receptor. The amino acid residues in the 5 Å surrounding the ligand benzoyl-L-arginine amide of 1WDA was defined as binding site. In Dock Ligands (CDOCKER) parameter settings, 1WDA: 1WDA was input as receptor, molecule: All was input as ligands, then the Top Hits was set to 10 and the Pose Cluster Radius to 0.5. The program was run to perform the docking calculations in Discovery Studio 4.0. The results were displayed by scoring docked ligand poses and analyzing interactions between small molecules and proteins.

3.2.2 Nanoscale self-assembly properties

The aqueous ZD-B and ZD-E-1 (0.05 mg/mL, pH 6.5 and 7.4) were dripped onto a formvar-coated copper grid (Euromedex, Souffelweyersheim, France). After thorough drying in air, the copper grid was kept in the dryer for 48 h. The shape and size of nanoparticles were observed with a transmission electron microscopy (TEM, JSM-6360 LV; JEOL, Tokyo, Japan) and a scanning electron microscopy (SEM, 50 kV; JEM-1230; JEOL).

The particle size and surface zeta potential of the particles in ultrapure water of pH 6.5 and pH 7.4 were measured using a dynamic light scattering (DLS) model and a BIC zeta potential analyzer (ZetaPlus S/N 21394; Brookhaven Instruments Corporation, Holtsville, NY, USA). The measurement was repeated for three runs per sample. The potential change for 6 days was recorded once every two days.

3.2.3. FT-MS spectrum

The nanodrugs were dissolved in a methanol/water (1:1) solution. Mass spectra were recorded on a Bruker 9.4 T SolariX FT-ICR mass spectrometer equipped with an ESI/MALDI dual ion source in positive and negative ion modes. Data were acquired using the SolariX control software. Spectral data were processed using the Bruker Daltonics data analysis software (Bruker Corp).

3.2.4. Molecular dynamics simulation

The nanodrugs were defined as an amphiphilic molecule in molecular dynamics simulations using Materials Studio. In a cubic box of $20 \times 20 \times 20$ Å, models of ZD-B and ZD-E-1 were distributed randomly with a density of 0.5 g/cm^3 . A 15,000 ps simulation was performed on this system at 298 K using the NVT ensemble.

3.2.5. NOSEY 2D NMR spectrum

NOSEY 2D NMR spectra were recorded on a Bruker 800 MHz spectrometer. The nanodrugs were dissolved in 400 µL of deuterated dimethyl sulfoxide containing 100 µL of deuterated water (D_2O). A trace amount of trifluoroacetic acid was used to adjust the pH of the solution to 6.5.

3.2.6. PAD4 inhibition

The inhibitory effect of PAD4 inhibitor was determined by a colorimetric method of inhibiting PAD4 catalyzed citrullination of BAEE (*N*α-benzoyl-L-arginine ethyl ester). Firstly, eight concentrations of inhibitors (60000, 20000, 6750, 2250, 750, 250, 85, 30 nmol/L) should be formulated with high purity water containing 1% DMSO. In a 96-well plate, 10 µL 10 × buffer (625 µL 1 mol/L pH=7.6 Tris-HCl, 25 µL 2 mol/L CaCl_2 , 50 µL 1 mol/L DTT, 125 µL 100 mmol/L PMSF, 425 µL H_2O) and water, then 20 µL inhibitor and 10 µL enzyme were added successively according to the different groups, incubated for 60 min at 37 °C, rpm = 400 (Eppendorf 5810R, Hamburg, Germany). The reaction was started by the addition of 10 µL 20 mmol/L BAEE aqueous solution (1 × buffer to dissolve), incubated for 90 min at 37 °C, rpm = 400 (Eppendorf 5810R), and quenched by the addition of 25 µL 5 mol/L HClO_4 , then transfer 125 µL of the reaction liquid to the corresponding label PE tube. 125 µL of Reagent A (0.2 g diacetyl monoxime and 0.6 g NaCl in 40 mL H_2O) and 250 µL of Reagent B (0.2 g antipyrine, 60 mg FeCl_3 , 10 mL H_2SO_4 and 10 mL H_3PO_4 in 20 mL H_2O) was added, respectively, to the above PE tube. It was then boiled at 100 °C for 30 min, cooled down in ice bath for 5 min, and then sucked back into the 96-well plate (250 µL per well) to observe the corresponding absorption value at 465 nm.

3.2.7. In vitro cytotoxicity

The cytotoxicity against cancer cells and HL7702 cells were studied by the MTT method. Cells were treated with different concentrations of compounds for 48 h in a 96-well plate. The MTT reagent (5 mg/mL) was added to each well subsequently and incubated for 4 h. Then the

culture medium was removed and residue was dissolved by DMSO. The optical density (OD) was read with Spectra Max M3 microplate reader (BioTek, Winooski, VT, USA) at 570 nm. The optical density value of treated wells was compared with that of control-treated wells. The proliferation of cancer cell lines or HL7702 cell lines were represented with IC₅₀. Each measurement was performed in triplicate. Data are presented as mean ± SD.

3.2.8. Western blotting analysis

The protein in cells was extracted according to instructions of Protein Extraction Kit (GenePool, GPP1814). According to the molecular weight of target protein, 12% (SQSTM1/p62), 15% (LC3B, H3cit) separate glue and 5% concentrate glue were prepared. After quantification of the protein, 60 µg of protein sample was added to each pore of SDS-PAGE gel electrophoresis. Then transferred to PVDF membrane. The membrane was blocked with 5% milk blocking buffer for 1 h. Then the membrane was incubated with antibodies at 4 °C for overnight. And the secondary antibody labeled by HRP was incubated for 1 h. The PVDF membrane was immersed in the ECL chromogenic solution (GenePool, GPP1824) for 1 min and exposed in the dark chamber. The gray value of band was read by Quantity One v.4.62 software. Antibodies used in the experiments were LC3B antibody (CST, 2775), SQSTM1/p62 antibody (CST, 5114), H3cit antibody (Abcam, ab5103), Goat Anti-Mouse IgG, HRP (Abcam, ab6789), Goat Anti-Rabbit IgG, HRP (Abcam, ab6721), and anti-β-actin antibody (Abcam, ab6276).

3.2.9. Transwell assay

100 µL of serum-free DMEM medium was added into the upper chamber, and 5×10^5 4T1 cells were seeded in each well after starvation treatment for 8 h. 600 µL of medium containing 10% serum was added to the lower chamber. Then ZD-E-1, 10 µmol/L RGDS, and PBS were added into the well, respectively. The final concentration of ZD-E-1 was 10, 5 and 2 µmol/L. After 24 h, the medium in upper chamber was removed and the chamber was washed twice, 4% paraformaldehyde was used to fix the cells for 30 min, and crystal violet was added for 15 min to stain the cells. The pictures from nine different fields were captured using a light microscope (Zeiss). The number of cells passing through the chamber was counted by ImageJ and represented as mean ± SD.

3.2.10. Cell morphology under TEM and SEM

The 4T1 cells were treated with 10 µmol/L ZD-E-1 for 48 h. The TEM samples were

collected in a 1.5 mL centrifuge tube. The SEM samples were cultured on sterilized coverslips placed in wells. Finally, 2.5% glutaraldehyde was added and fixed for 24 h at 4 °C. All samples were conducted by the Center Laboratory Morphology Platform at Capital Medical University in Beijing. Tecnai G2 transmission electron microscopy (Hitachi) and S-4800 scanning electron microscopy (Hitachi) was used to observe the shape of 4T1 cells.

3.2.11. Distribution in tumor tissues and its effect on H3cit

After removing the tumor from the mice, it was quick-frozen with liquid nitrogen. Embedded tissues with optimal cutting temperature compound were made as frozen sections. The sections were treated with 5% milk blocking buffer for 1 h. Then the sections were incubated with H3cit antibody (abcam: ab5103) at 4 °C for overnight. Finally, the sections were incubated for 1 h with secondary antibody, exposed to DAPI for 5 min in the dark, and observed by Slice Scanner.

3.2.12. Drug distribution in ICR mice

The fluorescence of ZD-B and ZD-E-1 *in vivo* could not be detected by a fluorescence imaging system (FX Pro KODAK). Thus, S180 tumor-bearing mice were sacrificed after 0.5, 2, 8 and 24 h, and the fluorescence of their organs was measured *ex vivo*.

3.2.13. Immunofluorescence and immunohistochemistry

After the tumor tissues were removed from the mice, they were immediately fixed in 4% paraformaldehyde solution, and paraffin sections were prepared. The paraffin sections were dewaxed to water and the antigen was repaired. The paraffin sections were treated for 1 h with 5% milk blocking buffer. Then the sections were incubated with antibodies at 4 °C overnight. The sections were then incubated with secondary HRP-conjugated antibody for 1 h and exposed to hematoxylin in the dark. Then, the paraffin sections were observed by Slice Scanner. The integral optical density (IOD) was calculated by Image-Pro Plus 6.0.

3.2.14. Critical aggregation concentration (CAC) of nanodrugs at different pH

The emission spectrum of Nile red shows a blue shift as the polarity of solvent decreased, which can be used for the determination of self-assembled molecule's CAC. First, 200 µmol/L Nile red was prepared with DMSO, then diluted with water to a concentration of 2 µmol/L (solution A). Second, the stock solutions (40 mmol/L) of ZD-B and ZD-E-1 were prepared with DMSO and diluted with water to a concentration of 400 µmol/L at pH 7.4 and pH 6.5.

The samples were then prepared to a series of concentrations (200, 100, 60, 40, 30, 20, 10, 2) with 1% DMSO at different pH values, sonicated for 30 min. Finally, the samples were mixed with equal volume of solution A and placed in the dark for 1 h before measurement. The emission spectrum of each solution was measured by a Shimadzu F2500 fluorescence spectrometer between 570 and 700 nm, using an excitation wavelength of 550 nm. The measurements were performed in triplicate. Intensity at 653 nm of solutions were obtained as a function of $\log[C]$.

3.2.15. *In vitro* drug release at different pH

The release of ZD-B and ZD-E-1 *in vitro* at different pH was evaluated by dialysis. 5 mL of nano-formulations (0.5 mg/mL) at pH 7.4 and pH 6.5 were placed in dialysis bags (Solarbio, 1 kD) and immersed in 50 mL of PBS (pH 7.4 and pH 6.5), respectively. The drug release was conducted on a shaker at 300 rpm (Eppendorf 5810R) and 37 °C. During dialysis, the aliquots (1 mL) were withdrawn from the release medium at predefined time intervals and replaced with an equal volume of fresh medium. The concentrations of released drug were determined by HPLC (Waters, e2695/2489, Milford, MA, USA; Xbridge C18 3.5 μ m, 4.6 \times 150 mm). Subsequently, the cumulative release curves were achieved.

3.2.16. Cellular uptake pathways

To determine the intracellular endocytosis pathway, we evaluated the cellular uptake of ZD-E-1 in the presence of clathrin-mediated endocytosis inhibitor chlorpromazine (30 μ mol/L), macropinocytosis inhibitor amiloride (50 μ mol/L), caveolae-mediated endocytosis inhibitor methyl- β -cyclodextrin (3 mmol/L) and blank medium. First, 4T1 cells were seeded in 6-well plates with 5×10^4 cells per well and three replicated wells in each group. After 12 h of culture, the medium was replaced with serum-free medium containing endocytic inhibitors for 1 h of incubation. Then, 250 μ L of ZD-E-1 (final concentration 20 μ mol/L) was added to each well and incubated for another 2 h. To measure the uptake pathways, cells were washed with cold PBS twice to remove the residual serum and drugs, digested with trypsin without EDTA and centrifuged at 1000 rpm (Eppendorf 5810R) for 5 min. Finally, the cells were washed and resuspended with 500 μ L of PBS, then analyzed by flow cytometry (BD) using FITC channel.

3.2.17. Uptake behavior at different pH

The uptake behavior of nanoparticles at different pH values were determined by HPLC-MS

(SCIEX, Xbridge BEH C18 2.5 μm , 2.1 \times 150 mm) and flow cytometry (BD). 4T1 and HL7702 cells were seeded in 10 cm dishes at 5×10^4 and 1×10^5 cells/mL, respectively, and incubated overnight. Each group was in triplicate. Then, the culture medium was replaced by fresh medium (pH 7.4 and pH 6.5), 2.5 mL of ZD-E-1 (final concentration 20 $\mu\text{mol/L}$) was added and incubated for 48 h. After incubation, the cells were washed and collected in 1 mL of PBS. Repeated freeze-thaw cycles followed by ultrasound to break up the cells. The cell suspensions were centrifugated at 12000 rpm (Eppendorf 5810R) for 10 min to obtain supernatant, and 9 mL of acetonitrile was added to precipitate the protein. It was then concentrated and re-dissolved with 1 mL of chromatographic acetonitrile. The contents of drugs were determined by HPLC-MS (SCIEX). The cellular uptake was also determined by flow cytometry (BD). In 6-well plates, ZD-B and ZD-E-1 were incubated with 4T1 cells at pH 7.4 and pH 6.5 for 48 h. Then, the cells were washed and collected in 500 μL of PBS. At least 1×10^4 cells were analyzed by flow cytometry (BD) using FITC channel.

3.2.18. The serum stability and pharmacokinetics

Serum from SD rats was used to determine the serum stability of ZD-E-1. 100 μL of 0.5 mg/mL ZD-E-1 was incubated with 900 μL of serum at 300 rpm (Eppendorf 5810R) and 37 $^{\circ}\text{C}$ for predefined time (5 min, 0.5, 1, 2, 3, 5, 8, 12, 24 and 48 h). Each group was performed in triplicates. Then, the serum proteins were precipitated with 9 mL of acetonitrile and sonicated for 15 min. After centrifugation at 12000 rpm (Eppendorf 5810R) for 15 min, the supernatants were diluted and analyzed by HPLC-MS (SCIEX).

The plasma pharmacokinetics of ZD-E-1 was determined in SD rats. After a single injection, blood samples were collected by the retro-orbital sinus at determined time (three samples per time point). The serums were obtained by centrifugation at 3000 rpm (Eppendorf 5810R) for 10 min, and 9 volume acetonitrile was added to precipitate protein. It was then sonicated and centrifugated at 12000 rpm (Eppendorf 5810R) for 10 min to get supernatant. The plasma drug levels were determined by HPLC-MS (SCIEX).

3.2.19 Single-cell mass cytometry analysis

Cells were cultured with cisplatin for 2 min to identify living cells. FIX I (Fluidigm, CA, USA) solution was used to fix the cells for 15 min. After three washes with CSB (Cell Staining Buffer, Fluidigm, CA, USA), cells were stained with an antibody cocktail against surface markers (Supporting Information Table S3) for 0.5 h at room temperature. Following three washes with CSB, cells were permeabilized with Perm-S (Fluidigm) and washed three

times with CSB; then, cells were subsequently stained with an antibody cocktail against intracellular markers. MaxPar barcoding Fluidigm was used to conjugate purified antibodies (table S3). All metal-conjugated antibodies were titrated for optimal concentration before staining cells. After three washes with CSB, cells were stained with iridium-containing DNA intercalator ($^{191}\text{Ir}/^{193}\text{Ir}$, final concentration of 125 nM) in FIX and Perm (Fluidigm, CA, USA) solution for 1 h at room temperature. Cells were then washed three times with double-distilled water and resuspended in 10% of EQ Four Element Calibration beads (Fluidigm, CA, USA) solution before detection with a Helios mass cytometer (Fluidigm, CA, USA). All normalized. fcs (Flow Cytometry Standard) files were uploaded to Cytobank (<https://www.cytobank.org/>) to finish data cleaning and analysis.